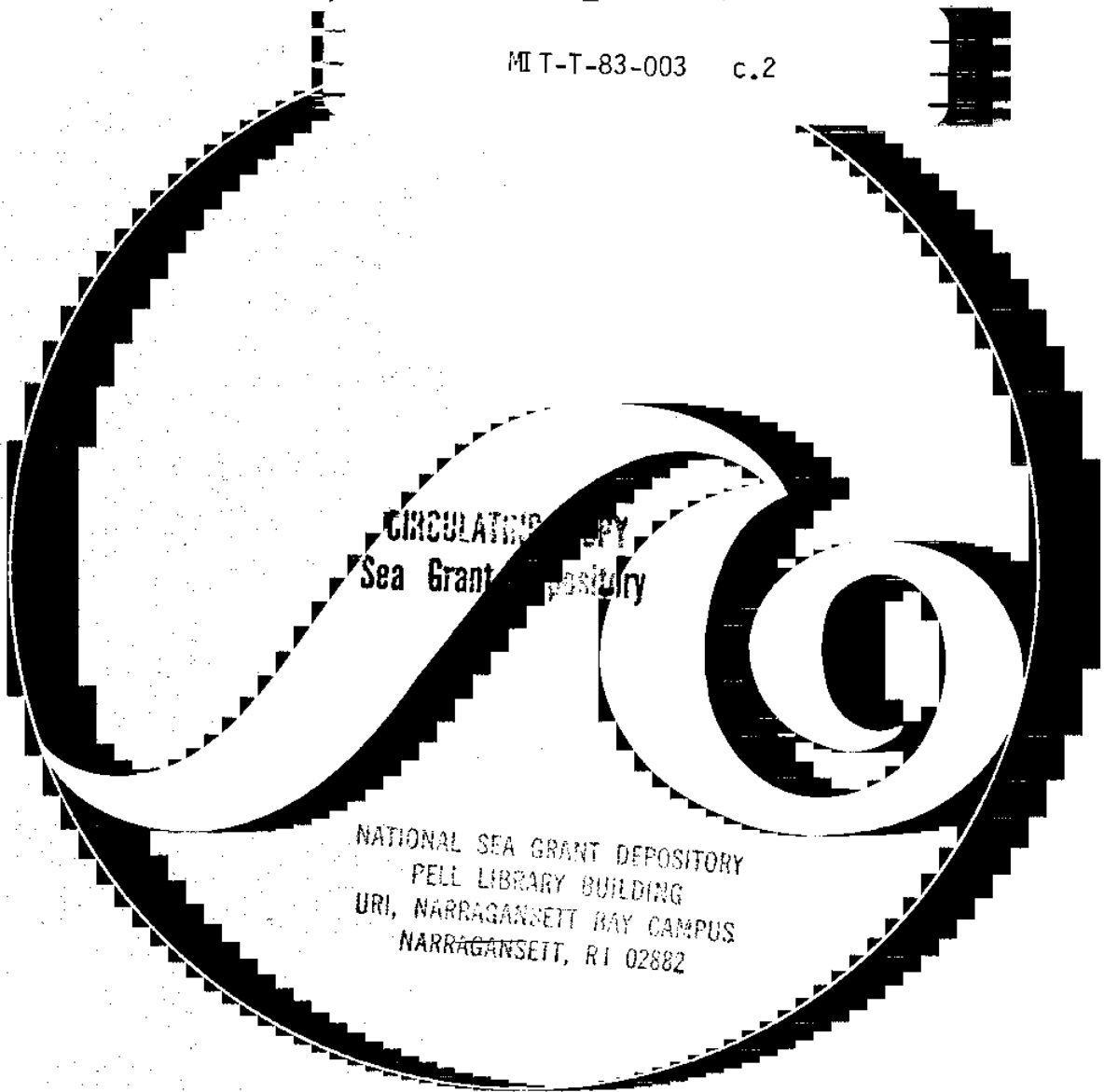


C. Chrysosostomidis
N.M. Patrikalakis

Theoretical and
Experimental Prediction
of the Response of a
Marine Riser Model
Subjected to Sinusoidal
Excitation of its Top End with
Amplitude of Two Diameters
Parallel to a Uniform Stream
of Speed Equal to 240 mm/s

MIT-T-83-003 c.2



MIT Sea Grant
Program

Massachusetts
Institute of Technology
Cambridge
Massachusetts 02139

Report Number
MITSG 83-4
March 1983



MASSACHUSETTS INSTITUTE OF TECHNOLOGY
Sea Grant Program

Addendum to MITSG 83-4, THEORETICAL AND EXPERIMENTAL PREDICTION OF THE RESPONSE OF A MARINE RISER MODEL SUBJECTED TO SINUSOID EXCITATION OF ITS TOP END WITH AMPLITUDE OF TWO DIAMETERS PARALLEL TO A UNIFORM STREAM OF SPEED EQUAL TO 240 mm/s

C. Chrysostomidis, N.M. Patrikalakis

Grant No. R/O-8
Project No. NA81AA-D-00069

**THEORETICAL AND EXPERIMENTAL
PREDICTION OF THE RESPONSE
OF A MARINE RISER MODEL
SUBJECTED TO SINUSOID EXCITATION
OF ITS TOP END WITH AMPLITUDE
OF TWO DIAMETERS PARALLEL
TO A UNIFORM STREAM OF SPEED
EQUAL TO 240 mm/s**

by

**C. CHRYSSOSTOMIDIS
N. M. PATRIKALAKIS**

MIT SEA GRANT REPORT NO. 83-4

MARCH, 1983

ABSTRACT

The objective of this report is to provide:

1. An analysis of the experimental results obtained from a 3 m flexible riser model with its top end oscillated harmonically with an amplitude of two diameters parallel to a uniform stream which is constant with depth and of speed equal to 240 mm/s.

2. A comparison of the experimental results from the flexible model with theoretical predictions of the response based on rigid cylinder experimental results.

ACKNOWLEDGEMENTS

Funding for this research was obtained from the MIT Sea Grant College Program, Conoco, Inc. and Gulf Oil Company. All experiments were performed at the Laboratory for Hydrodynamics of the National Technical University of Athens, Greece. The typed manuscript was prepared by M. Staruch.

RELATED SEA GRANT REPORTS

"Theoretical and Experimental Prediction of the Response of a Marine Riser Model Subjected to Sinusoid Excitation of its Top End with Amplitude Equal to Two Diameters," C. Chryssostomidis, N.M. Patrikalakis, and E. Vrakas, MIT Sea Grant Report No. 83-2, March 1983.

"Theoretical and Experimental Prediction of the Response of a Marine Riser Model Subjected to Sinusoid Excitation of its Top End with Amplitude of Two Diameters Parallel to a Uniform Stream of Speed Equal to 120 mm/s," C. Chryssostomidis and N.M. Patrikalakis, MIT Sea Grant Report No. 83-3, March, 1983

"Theoretical and Experimental Prediction of the Response of a Marine Riser Model Subjected to Sinusoid Excitation of its Top End with Amplitude of Two Diameters Orthogonal to a Uniform Stream of Speed Equal to 120 mm/s," N.M. Patrikalakis and C. Chryssostomidis, MIT Sea Grant Report No. 83-5, March, 1983.

"Theoretical and Experimental Prediction of the Response of a Marine Riser Model Subjected to Sinusoid Excitation of its Top End with Amplitude of Two Diameters Orthogonal to a Uniform Stream of Speed Equal to 240 mm/s," N.M. Patrikalakis and C. Chryssostomidis, MIT Sea Grant Report No. 83-6, March, 1983.

TABLE OF CONTENTS

	Page
Abstract	1
Acknowledgements	2
Table of Contents	3
List of Tables.	4
List of Figures	5
1. A Description of the Riser Model.	6
2. Presentation of Experimental and Theoretical Results	9
Experiment 9	14
Experiment 10	26
Experiment 8	38
Experiment 7	50
References	62
Appendix A	63

LIST OF TABLES

Table 2-1:	Description of experiments and information for the theoretical prediction of the response in plane A.	10
------------	---	----

LIST OF FIGURES

	Page
EXPERIMENT 9:	
-Spectra	14
-Theoretical predictions and maxima	22
-T-Figures.	24
EXPERIMENT 10:	
-Spectra	26
-Theoretical predictions and maxima	34
-T-Figures.	36
EXPERIMENT 8:	
-Spectra	38
-Theoretical predictions and maxima	46
-T-Figures.	48
EXPERIMENT 7:	
-Spectra	50
-Theoretical predictions and maxima	58
-T-Figures.	60
Figures A1 and A2:	
-Rigid cylinder results.	64

1. A DESCRIPTION OF THE RISER MODEL

Preliminary data describing the riser model can be found in Chryssostomidis and Patrikalakis (1982) and MITSG Report 83-2, and more refined estimates in Patrikalakis (1983). A description of the model based on the information given in Patrikalakis (1983) is included here for the reader's convenience.

The model is made up of an aluminum tube covered externally with a sealing material. The overall model characteristics are:

- Length between ball joints (L) = 3.000m
- Aluminum tube I.D. (D_i) = 10.92 mm
- Aluminum tube O.D. (D_o) = 12.61 mm
- External sealing diameter (D_e) = 15.3 mm
- Average mass per unit length (M) = 0.327 kg/m
- Average effective weight per unit length (We) = 1.378 N/m
- Effective overpull at the lower ball joint ($Pe(0)$) = 1.72 N
- Bending stiffness of a cross section (EI) = 37.6 Nm²

The inside of an aluminum tube is filled with a glycerin solution in water of density approximately equal to 900 kg/m³. At the ends of the model there are ball joints which minimize the end bending moments. Above the upper ball joint there is a slip joint, which is designed to minimize tension variations due to flexural motions. The riser model is also designed so it can be tensioned to the desired tension. The first two "natural frequencies" of the model in water are approximately equal to 1.57 and 6.06 Hz, respectively. These have been determined theoretically using $c_m=1$ and have been verified from a decay test in quiescent

water, where the initial amplitude of the response was of the order of $1/10$ of the effective diameter.

The model is instrumented at ten equidistant locations, 1-10, each with two strain gage full bridges installed on the outer surface of the aluminum tube, designed to isolate bending from tension and to measure bending strains on two orthogonal directions A and B. In the vertical static equilibrium condition, planes A and B are parallel and orthogonal to the centerline of the towing tank, respectively. The actual location of each branch of the bending bridges is at approximately 9.80 degrees from planes A and B. The numbering of the bridges begins at the upper end, while their elevation is measured from the axis of the lower ball joint. The first and last bending bridges are $L/11$ from the axes of the top and bottom ball joints, respectively, and the separation between bending bridges is $L/11$. For example, bridge A6 measures bending strains created by deflections in plane A at elevation $Z=5L/11$ from the axis of the lower ball joint. In addition, the model is instrumented at two extra positions T1 and T2, 101 mm from the axes of each ball joint, with specially designed full bridges isolating tension from bending. Tension bridge T2 is at the lower end of the model. Finally, the model is instrumented at an additional location, Q1, 1773 mm from the upper ball joint, with a full torsion bridge. The mass per unit length of a single wire is 0.198 grams/m, while the total mass of all wires for all 23 full bridges is approximately 2.73% of the total model mass. Their total volume is approximately equal to 5.32 cm^3 . The four wires of each bridge are braided to avoid interference and are sent internally to the lower end of the model.

The oscillation of the top end of the model is created by a DC motor driven by a signal generator and controlled by a tachometer measuring angular velocities and a linear variable differential transducer, LVDT, measuring displacements. The rotational motion of the motor is converted to linear motion via a specially designed rack anti-backlash pinion system. During the experiments, measurements

from a number of strain bridges and the LVDT were made simultaneously and were recorded digitally. Using the torque bridge, it was observed that the structural torsion was negligible, see Chapter III of Patrikalakis (1983). It was estimated analytically, and also confirmed by the tension bridge measurements, that the tension variation during the experiments was small, approximately 5% of the effective tension. Therefore, even for the lowest excited mode, the ratio of the change of restoring force due to tension variation to the overall restoring force is very small (0.3%). This implies that the assumption of constant effective tension with time is an acceptable approximation for theoretical estimates of the response.

From calibration experiments in air, it was estimated that the structural damping ratio ζ was approximately equal to 0.016 and 0.010 for the first and second flexural modes, respectively. Therefore, typical fluid drag forces are much larger than our estimates of the structural damping forces. Our experiments in air also revealed that when the upper end of the model was oscillated in air in a certain plane, some flexural response orthogonal to this plane existed. This happens because our model was not rotationally uniform. It was estimated that the flexural response orthogonal to the direction of excitation was not larger than approximately 12% of the response in the plane of applied oscillation. It was felt that such an imperfection would not substantially affect the experimental results in water.

2. PRESENTATION OF EXPERIMENTAL AND THEORETICAL RESULTS

The experiments presented in this report involve harmonic excitation of the top end of the riser model parallel to plane A at an amplitude approximately equal to two effective diameters and parallel to a uniform stream which is constant with depth and of speed V_c equal to 240 mm/s for the conditions shown in Table 2-1. Bending strains in plane A at $Z=3L/11$, $5L/11$ and $8L/11$, and in plane B at $Z=3L/11$, $6L/11$ and $8L/11$ were recorded. The Reynolds number and water temperature for all experiments analyzed in this report are 3040 and 13 degrees C, respectively. Reynolds number is defined by $Re = V_c D_e / \nu$ where ν is the kinematic viscosity of fresh water. A partial preliminary analysis of the experiments presented in this report has been given earlier in Chryssostomidis and Patrikalakis (1982).

The experimental and theoretical results reported here include plots of:

1. The root mean square of the measured motion of the top end as a function of frequency.
2. The root mean square measured dynamic bending strains as a function of the response frequency and the measured static bending strains.
3. The measured and theoretical predictions of the bending strains parallel to the oscillation of the top end.
4. The measured maximum bending strains parallel and orthogonal to the oscillation of the top end and independent of direction.
5. Indicative partial synchronous time traces of the motion of the top end and measured bending strains from three bridges.

The root mean square responses have been calculated using standard FFT codes from the International Mathematical and Statistical Library (IMSL) on an IBM 370/168 computer. The root mean square response is the square root of the

Table 2-1: Description of experiments and information for the theoretical prediction of the response in plane A

Experiment Number	9	10	8	7
Frequency of Excitation f_e in Hz	1	1.5	2.3	3
Measured A/D_e	2.03	2.01	2.04	2.04
Reduced Velocity U^*	15.68	10.03	6.82	5.22
Reduced Frequency β	194	291	446	582
Measurement Record Length in Seconds	34.1	34.1	34.1	17.05
Added Mass Coefficient \hat{c}_m Used in Theoretical Prediction	0.53	0.47	0.47	0.45
Drag Coefficient \hat{c}_d Used in Theoretical Prediction	1.02	1.07	1.10	1.20
Maximum Calculated Dynamic Displacement Ratio x/D_e	2.03	2.01	2.04	2.04
Mean Calculated Dynamic Displacement Ratio x/D_e	1.20	1.31	0.92	0.79

product of the power spectral density of the response times the effective bandwidth B_e employed in the Fourier analysis of the results. The root mean square rather than the magnitude of the power spectral density was selected for presentation because, in most cases, the experimental response was practically periodic. The logarithmic representation of the power spectral density was not selected because it tends to visually exaggerate the significance of smaller components, which are not important in this problem. For each major peak of the root mean square plots, the root mean square value of the response is shown. This is computed as the square root of the sum of the squares of the rms response strains at discrete frequencies, B_e Hz apart, in the neighborhood of each peak. In addition, the overall dynamic root mean square value of the response is shown together with the static bending strain response. The Fourier and maxima calculations were performed using the record length shown in Table 2-1.

The nomenclature used in the Figures and Table 2-1 is defined below:

The experiment number corresponds to the numbering system employed during the performance of the experiments. BE is the effective bandwidth B_e employed in the Fourier analysis in Hz. THETA is the angle of oscillation of the top end with respect to the longer side of the towing tank in degrees. VC is the current speed V_c in mm/s. FE is the nominal frequency of excitation f_e of the top end in Hz. A/DE is the ratio of the measured amplitude A of the excitation of the top end divided by the effective diameter D_e . U^* is the reduced velocity defined by $U^* = V_c / f_e D_e$ and β is the frequency parameter defined by $\beta = f_e D_e^2 / \nu$.

The Figures of the root mean square motion of the top end are referred to by the experiment number and the letters LVDT. The Figures of root mean square measured bending strains are referred to by the experiment identification number and the bridge name. The Figures showing the measured and theoretical predictions and maxima are referred to by the experiment identification number

and the plane name. Figures showing the time traces are referred to by the experiment identification number and the letter T (trace).

Table 2-1 includes information about the theoretical prediction of the response at $f=f_e$ in plane A, performed as described in Section IV.4.4 of Patrikalakis (1983). The procedure for computing \hat{c}_m and \hat{c}_d shown in Table 2-1 can be found in Section IV.4.4 and Appendix B of Patrikalakis (1983). The estimates of the local c_m and c_d employed in the iteration procedure are based on Figures A1 and A2 taken from Verley and Moe (1979). The frequency parameter β in our experiments varied between 194 and 582, which for the most part overlaps with the range of β employed by Verley and Moe (1979).

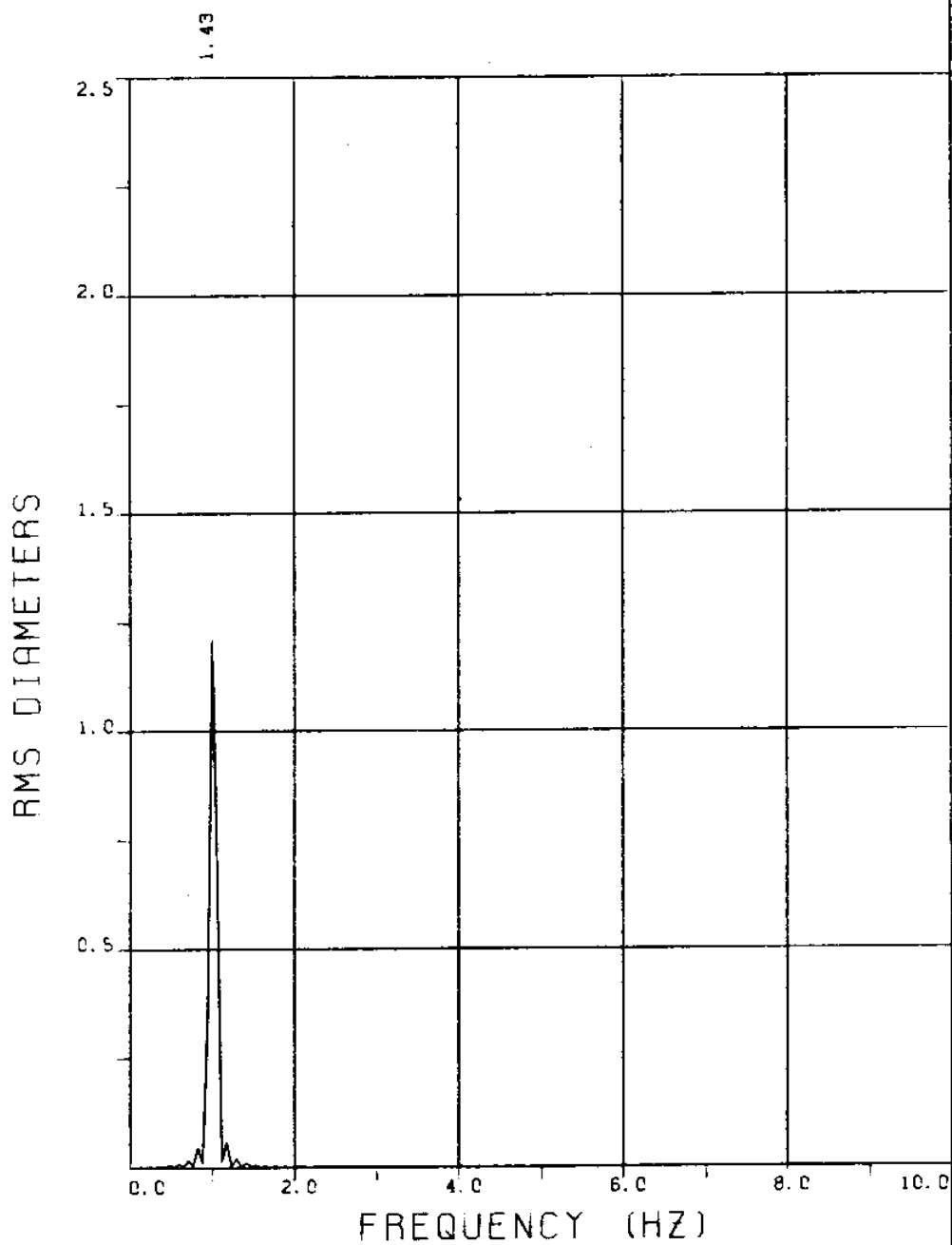
From all experiments of this class, it can be seen that the strain response in plane A is primarily concentrated at $f=f_e$, as expected from rigid cylinder results. However, some strain response in plane A at frequencies other than f_e exists and is not, in general, insignificant in determining the maxima of the measured response in plane A. These results are summarized in Figures 9A, 10A, 8A and 7A, where the theoretical and measured static and static plus dynamic response strain at $f=f_e$ and the measured maximum response strain in plane A are shown. The theoretical static plus dynamic response strain at $f=f_e$ in plane A is also our theoretical estimate for the maximum response strain in this plane. In general, the responses in plane B are as significant as the dynamic responses in plane A. The frequencies at which there is significant lift response depend upon the value of U^* , see Chryssostomidis and Patrikalakis (1983). For all experiments analyzed in this report the value of U^* is larger than 3 and significant lift response occurs at multiples of $f_e/2$. This is consistent with rigid cylinder results, Mercier (1973). It may also be of interest to note that the Strouhal frequency determined using the current alone does not appear to be an important parameter in the type of flow studied here. For example, the experimentally determined value of the Strouhal frequency for our model was found to be $f_r=2.14$ Hz and no appreciable lift

response was observed at this frequency except for experiment 10 for which $f_r \simeq 3f_e/2$.

These results are summarized in Figures 9B, 10B, 8B and 7B where the maximum measured dynamic response strain in plane B and the maximum measured static and dynamic response strain independent of plane are shown. At present, our theoretical estimate of the maximum static and dynamic response strain independent of plane is the same as our theoretical estimate of the static plus dynamic response strain at f_e in plane A, because no information is available to us to make an estimate of the magnitude of the lift response. The theoretical estimate of the maximum independent of plane is also shown in the "B" Figures.

Finally, the "T" Figures of each experiment are included to allow the reader to roughly estimate the phase between the excitation of the top end and the response.

EXPERIMENT 9

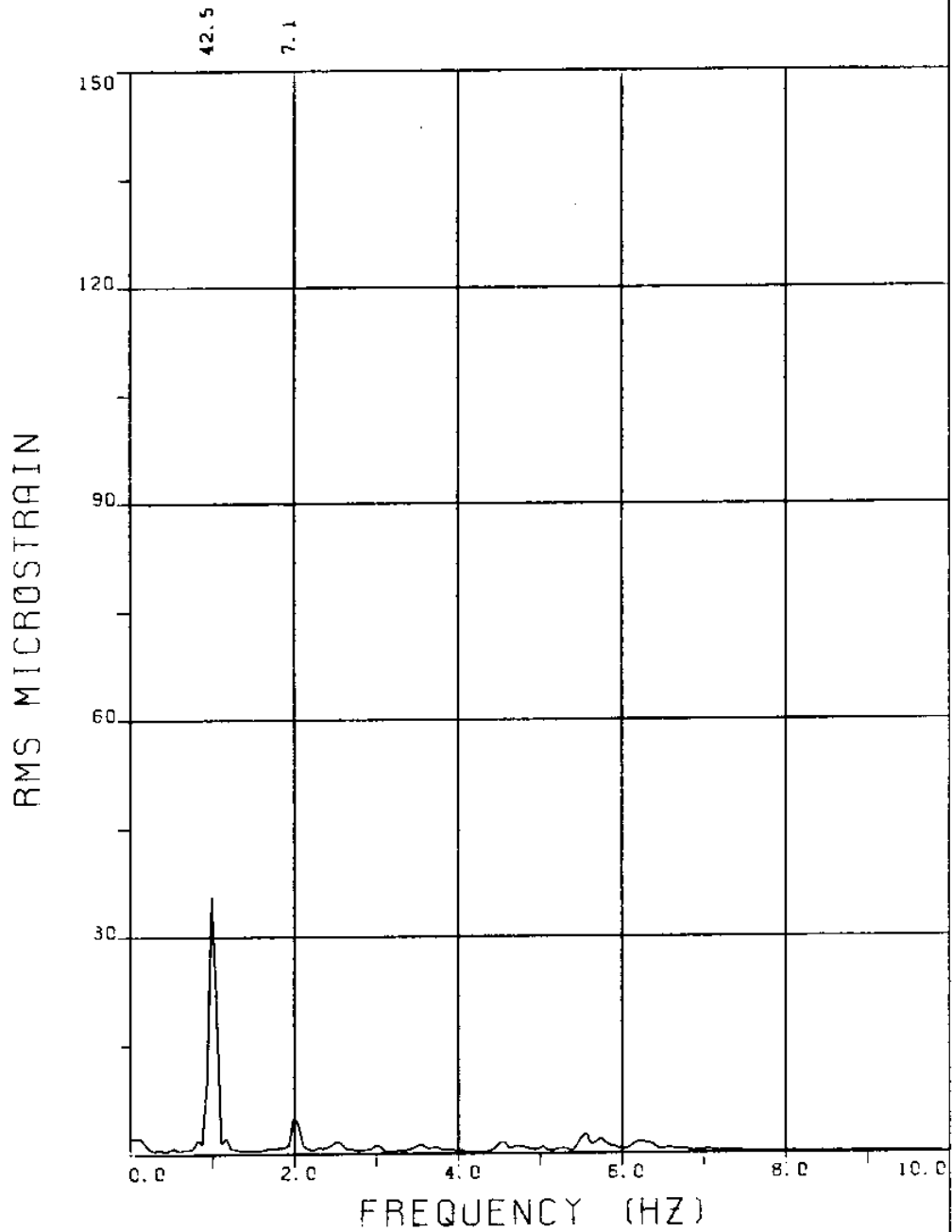


EXPERIMENT NUMBER 9

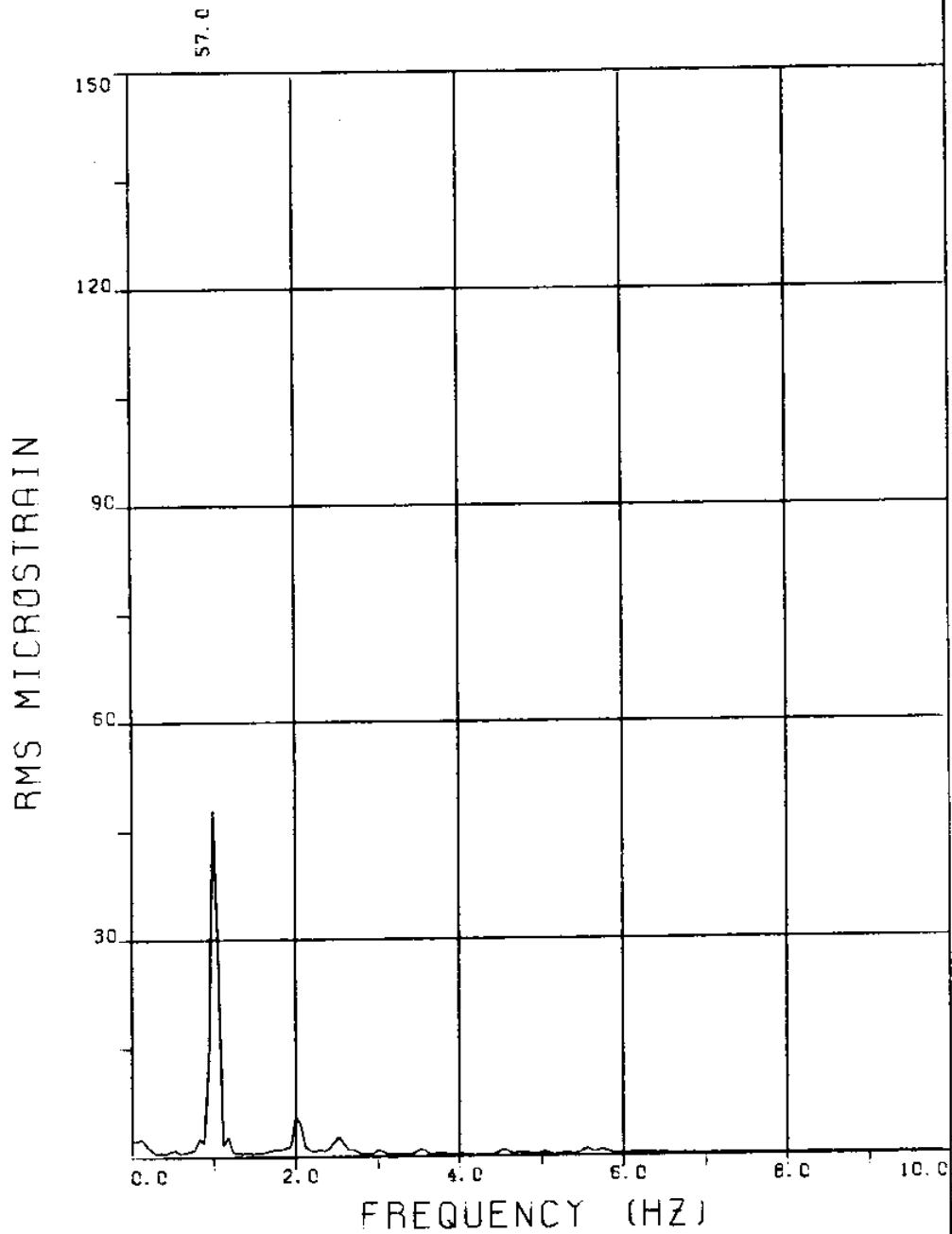
LVDT

THETA=0 VC=240 FE=1.000 BE=0.059

MEASURED A/DE=2.03



EXPERIMENT NUMBER 9
BRIDGE A8 ELEVATION=3L/11 BE=0.059
THETA=0 VC=240 FE=1.000 A/DE=2.03
MEASURED RESPONSE IN MICROSTRAIN
MEAN=87.9
TOTAL DYNAMIC RMS=44.0



EXPERIMENT NUMBER 9

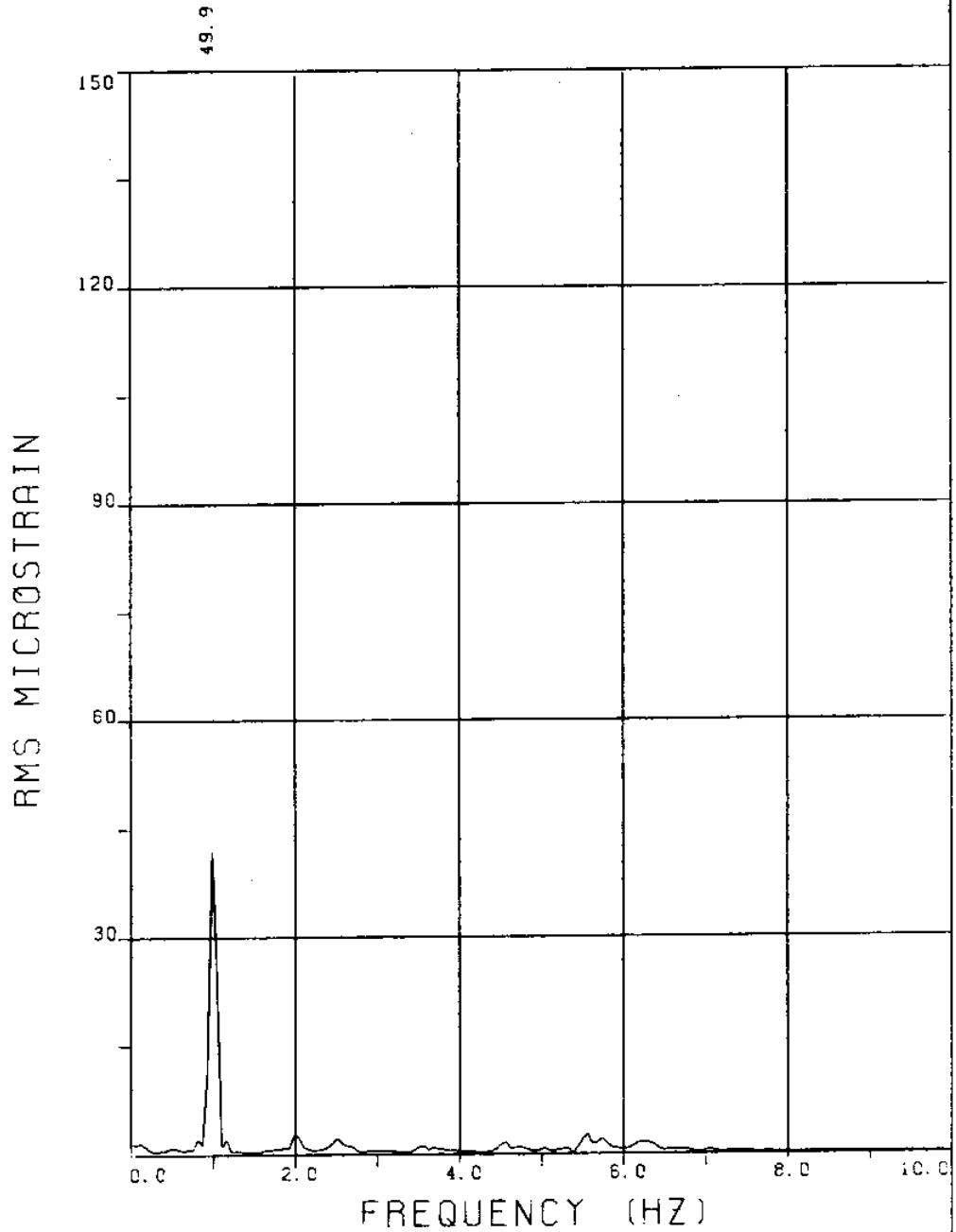
BRIDGE A6 ELEVATION=5L/11 BE=0.059

THETA=0 VC=240 FE=1.000 A/DE=2.03

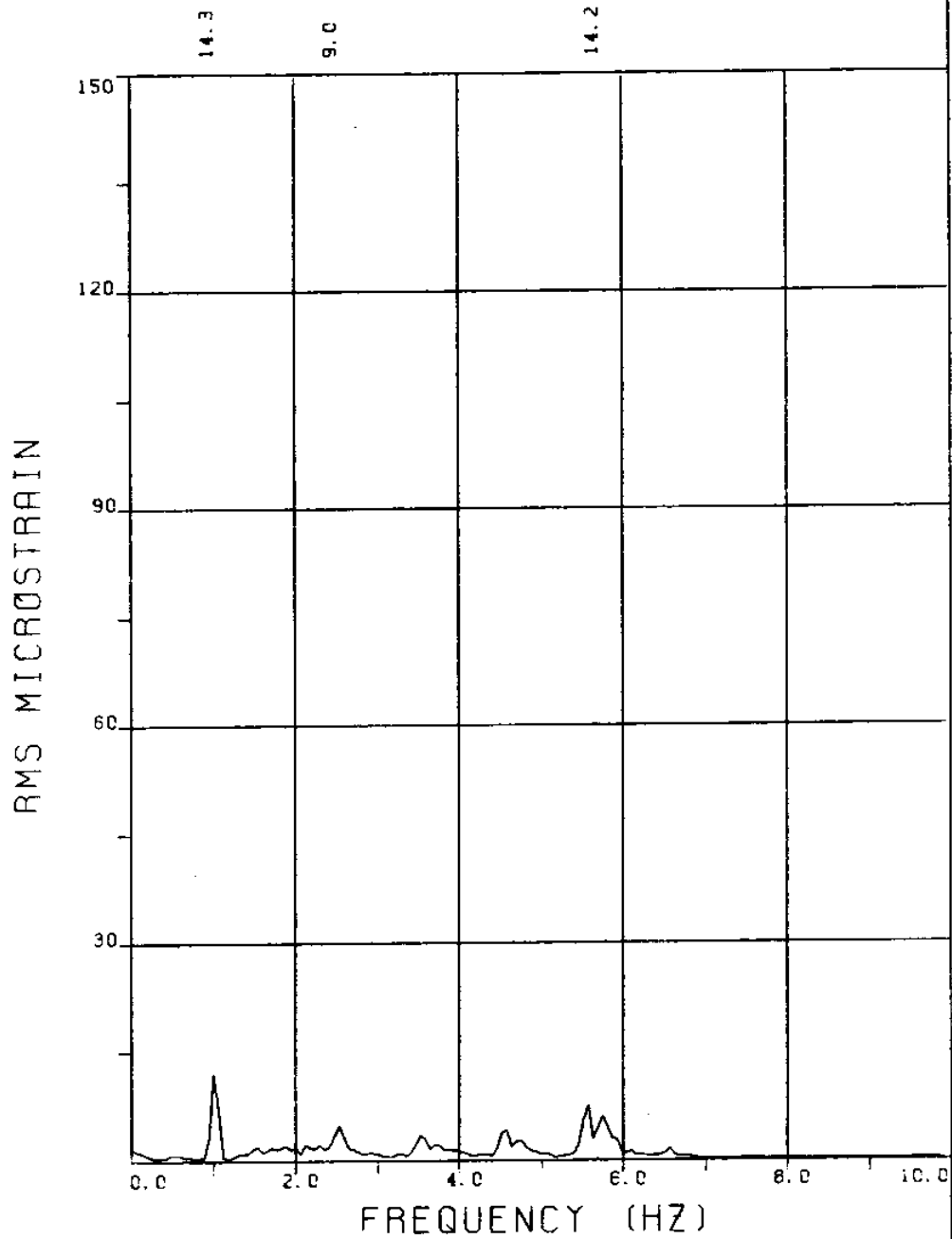
MEASURED RESPONSE IN MICROSTRAIN

MEAN=107.8

TOTAL DYNAMIC RMS=58.0



EXPERIMENT NUMBER 9
BRIDGE A3 ELEVATION=8L/11 BE=0.059
THETA=0 VC=240 FE=1.000 A/DE=2.03
MEASURED RESPONSE IN MICROSTRAIN
MEAN=92.8
TOTAL DYNAMIC RMS=50.9



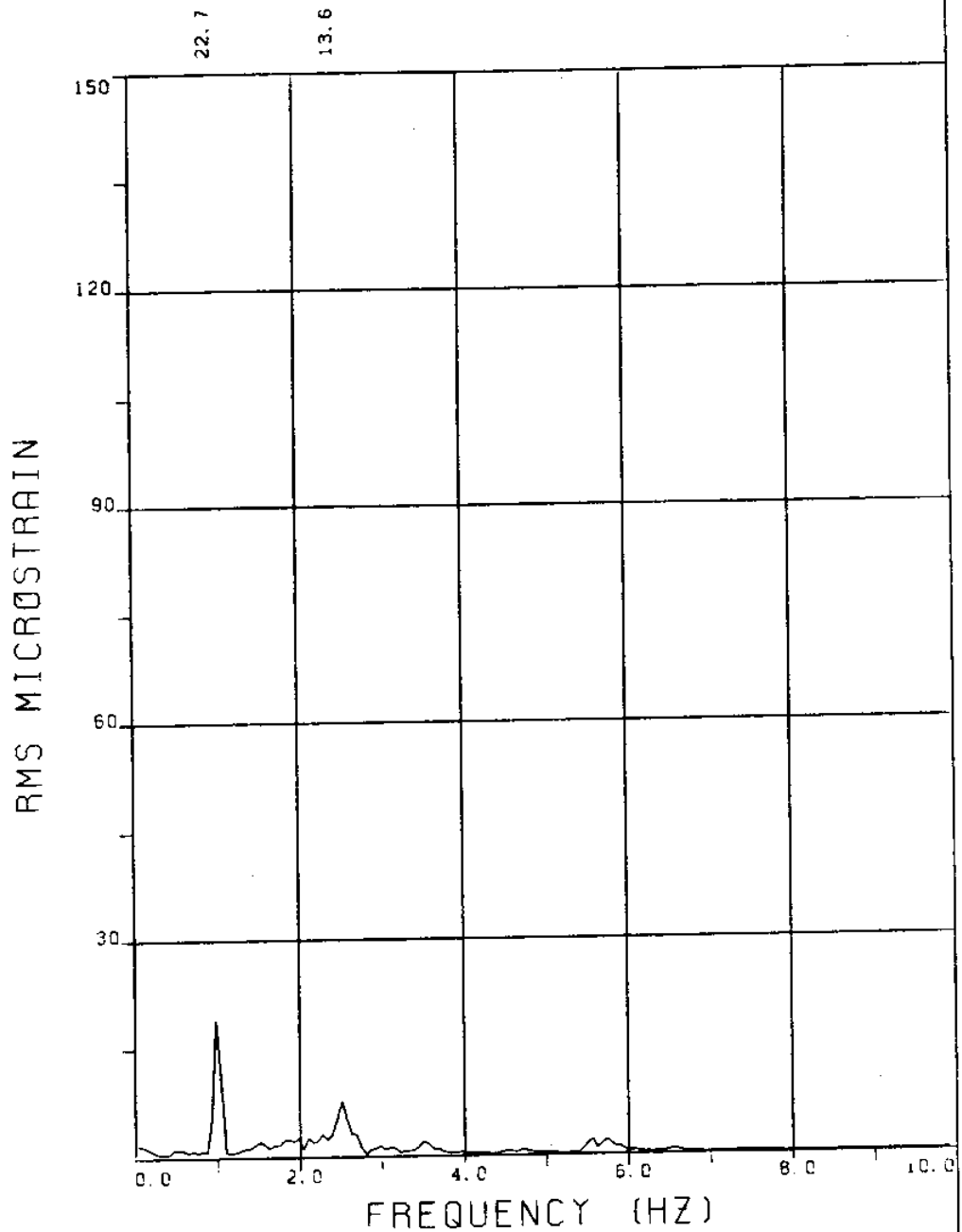
EXPERIMENT NUMBER 9

BRIDGE B8 ELEVATION=3L/11 BE=0.059

THETA=0 VC=240 FE=1.000 A/DE=2.03

MEASURED RESPONSE IN MICROSTRAIN

TOTAL DYNAMIC RMS=25.3



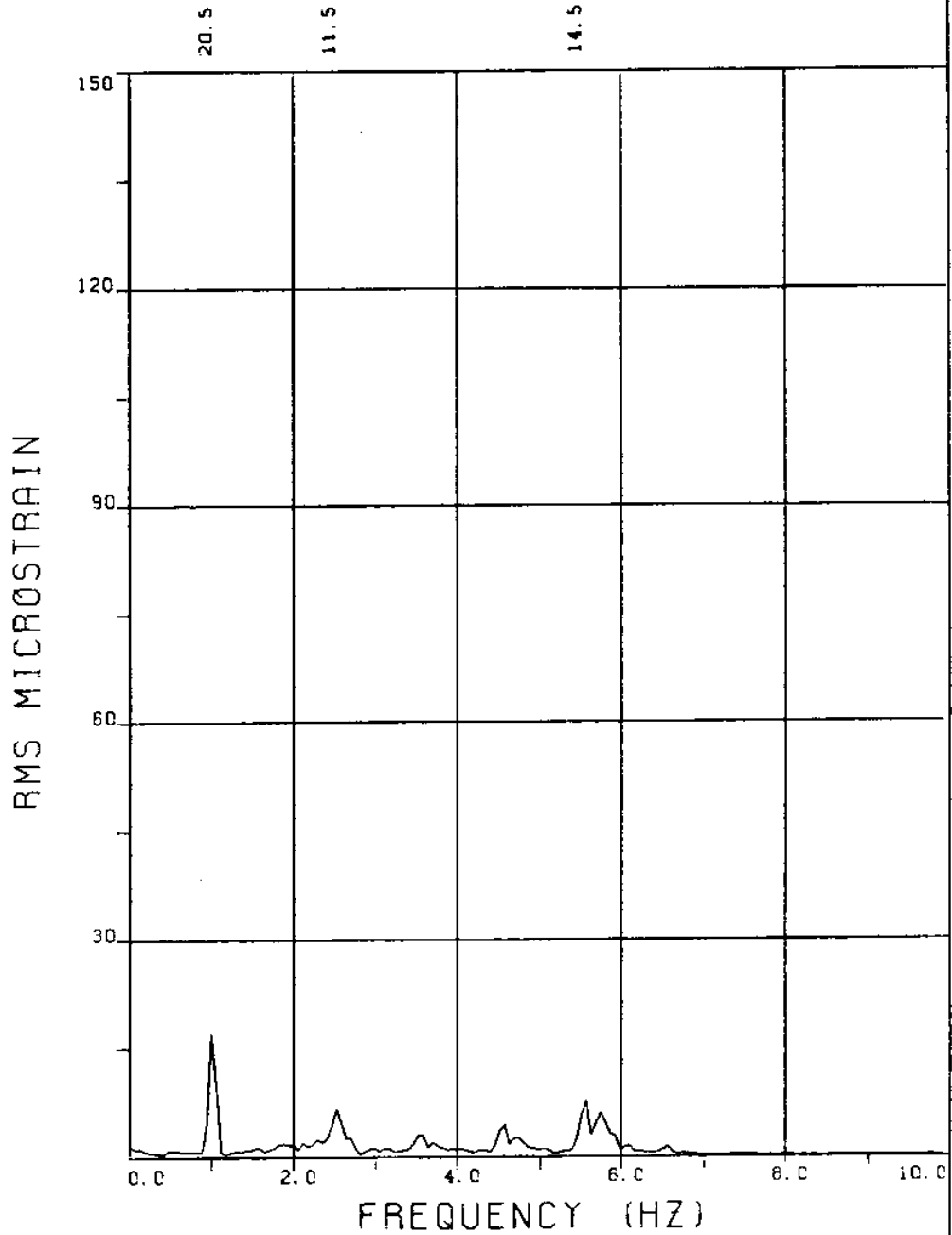
EXPERIMENT NUMBER 9

BRIDGE B5 ELEVATION=6L/11 BE=0.059

THETA=0 VC=240 FE=1.000 A/DE=2.03

MEASURED RESPONSE IN MICROSTRAIN

TOTAL DYNAMIC RMS=27.9



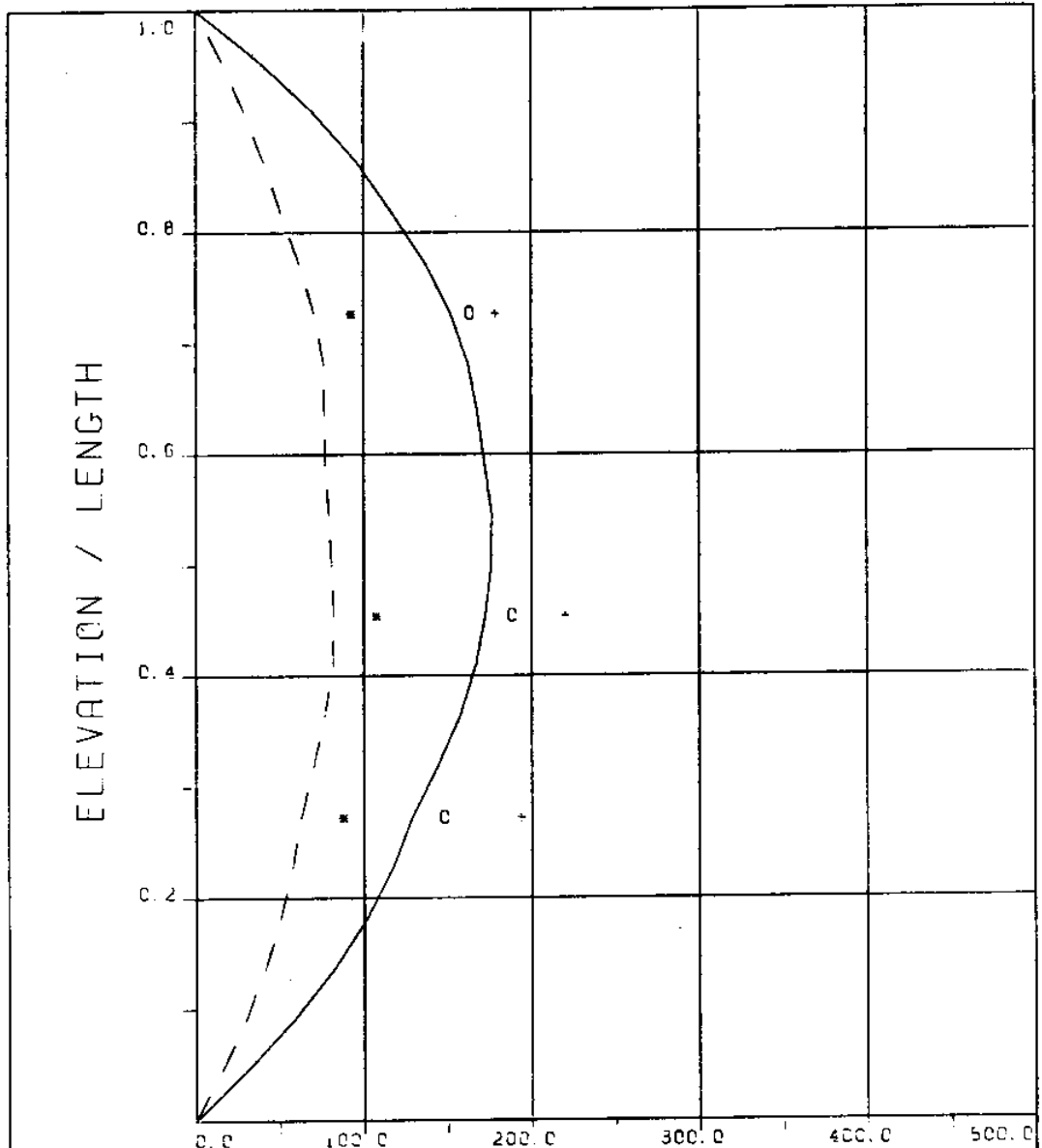
EXPERIMENT NUMBER 9

BRIDGE B3 ELEVATION=8L/11 BE=0.059

THETA=0 VC=240 FE=1.000 A/DE=2.03

MEASURED RESPONSE IN MICROSTRAIN

TOTAL DYNAMIC RMS=30.0



MICROSTRAIN

EXPERIMENT NUMBER 9

THETA=0 VC=240 FE=1.000 A/DE=2.03

STATIC RESPONSE IN PLANE A

----- THEORY * * * EXPERIMENT

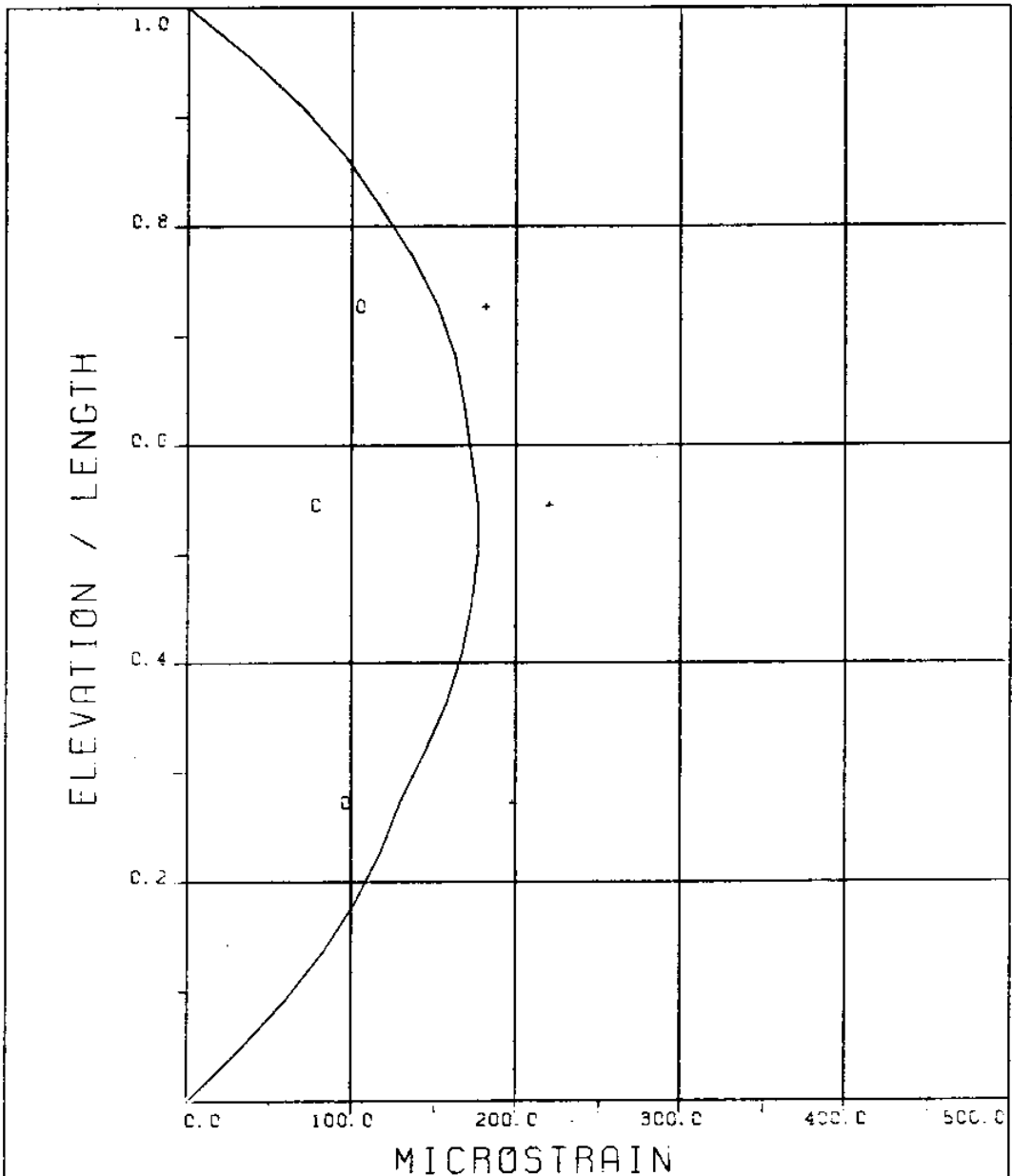
STATIC RESPONSE PLUS DYNAMIC

RESPONSE AT $F = F_E$ IN PLANE A

_____ THEORY o o o EXPERIMENT

MAXIMUM RESPONSE IN PLANE A

_____ THEORY + + + EXPERIMENT



EXPERIMENT NUMBER 9

THETA=0 VC=240 FE=1.000 A/DE=2.03

MAXIMUM DYNAMIC RESPONSE IN PLANE B
 o o o EXPERIMENT

MAXIMUM RESPONSE
 _____ THEORY + + + EXPERIMENT

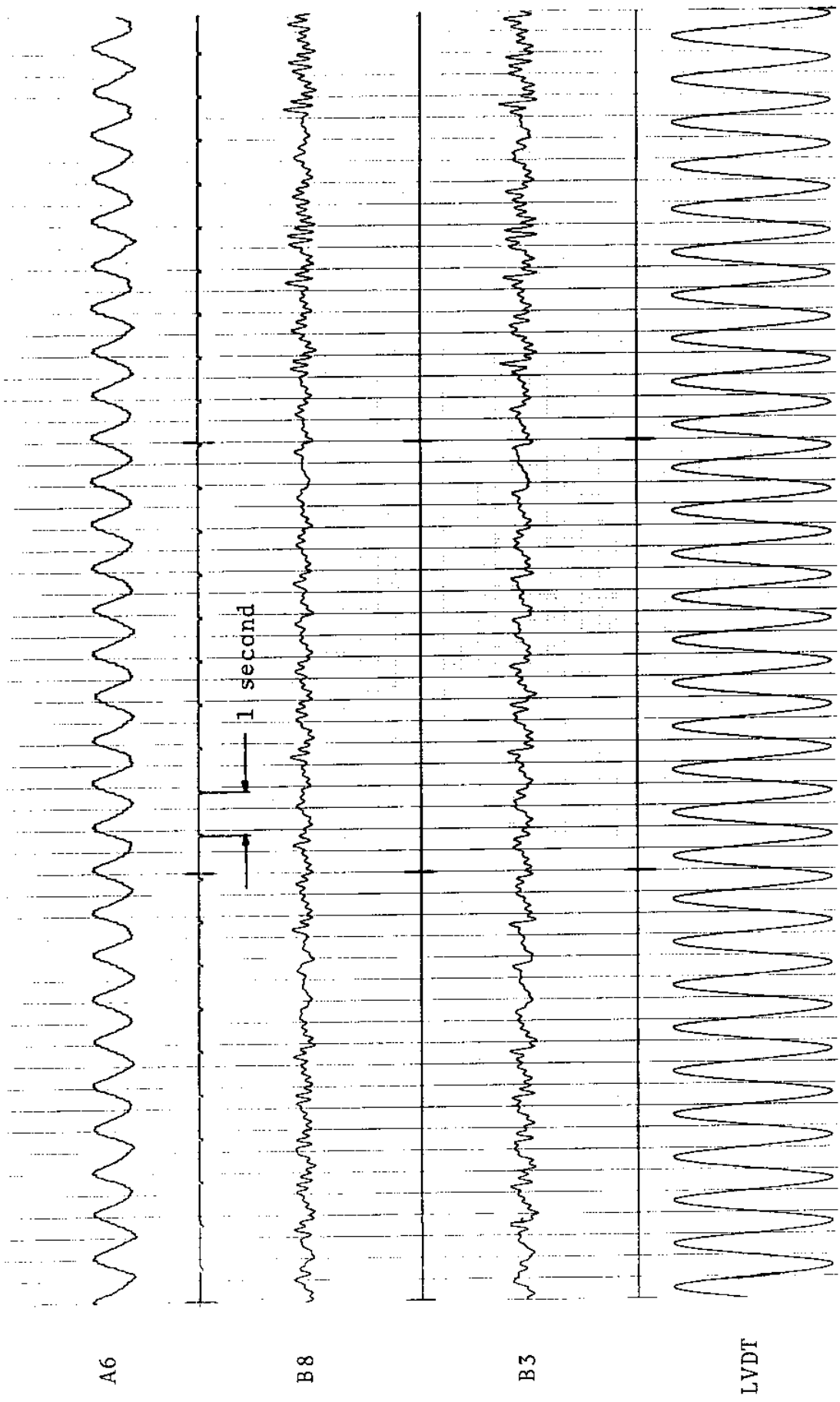


FIGURE 9Ta: LVDT: 0.087 D_e/DIVISION; STRAINS: 15.3 MICROSTRAIN/DIVISION

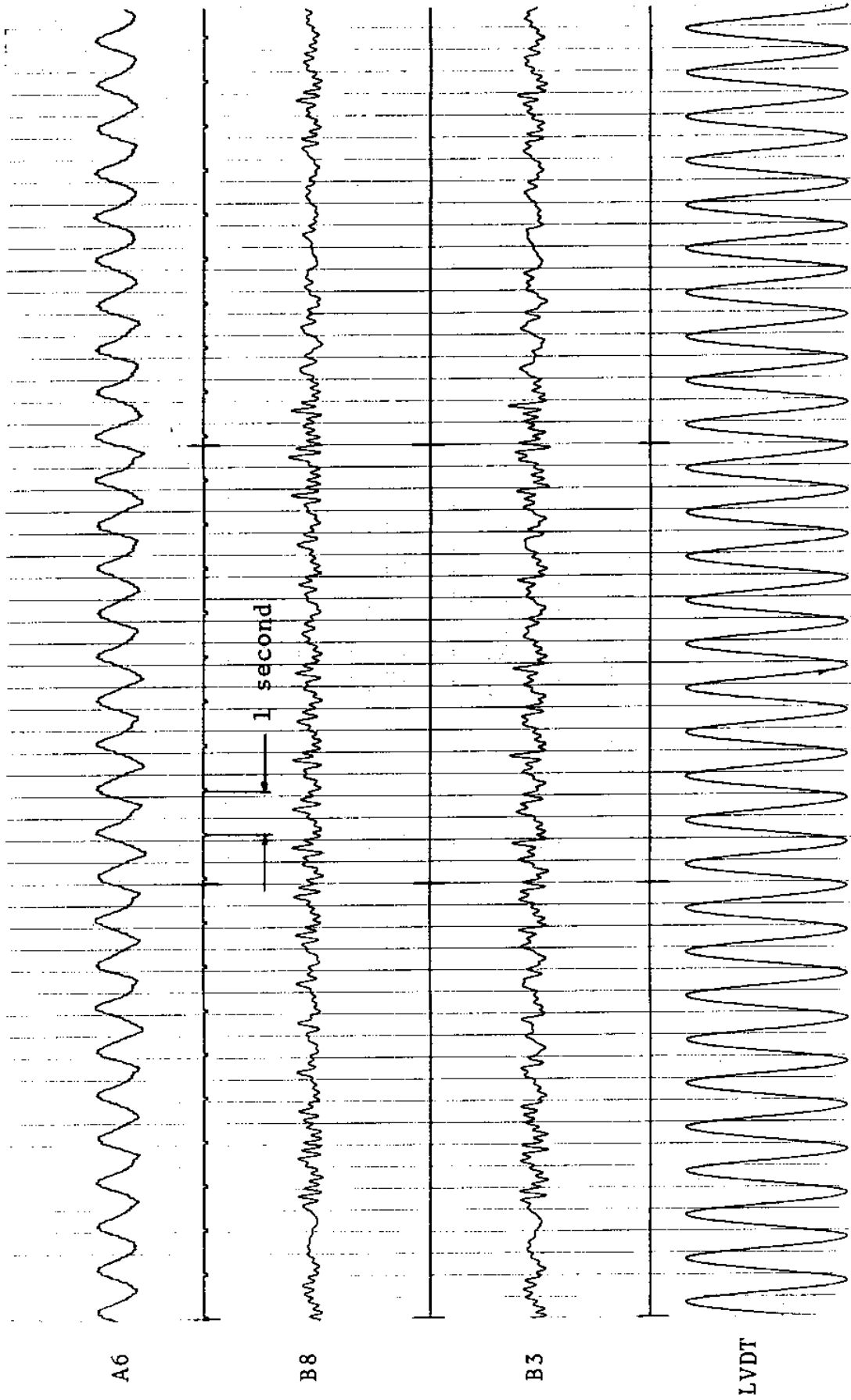
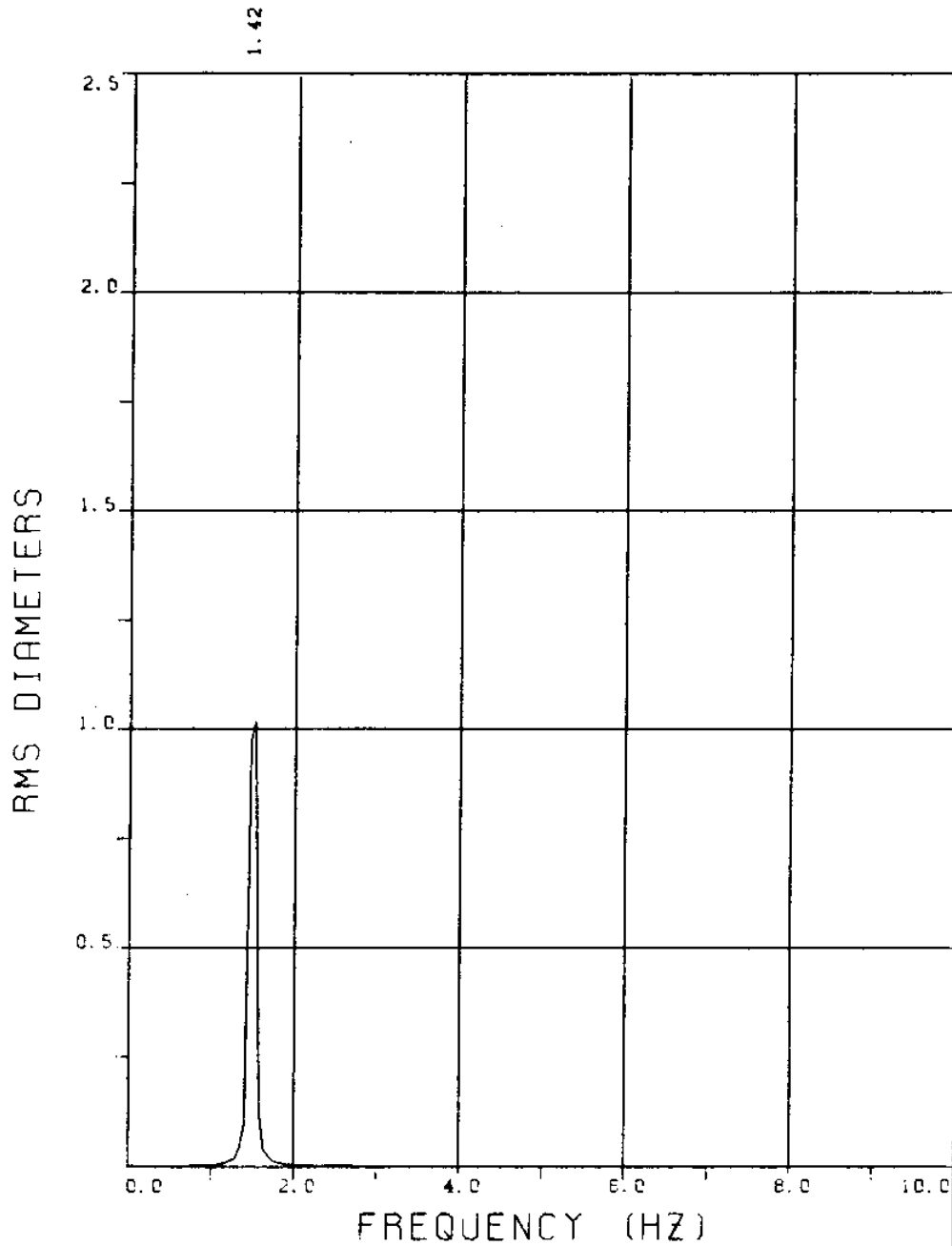


FIGURE 9Tb: LVDT: 0.087 D_e/DIVISION; STRAINS: 15.3 MICROSTRAIN/DIVISION

EXPERIMENT 10

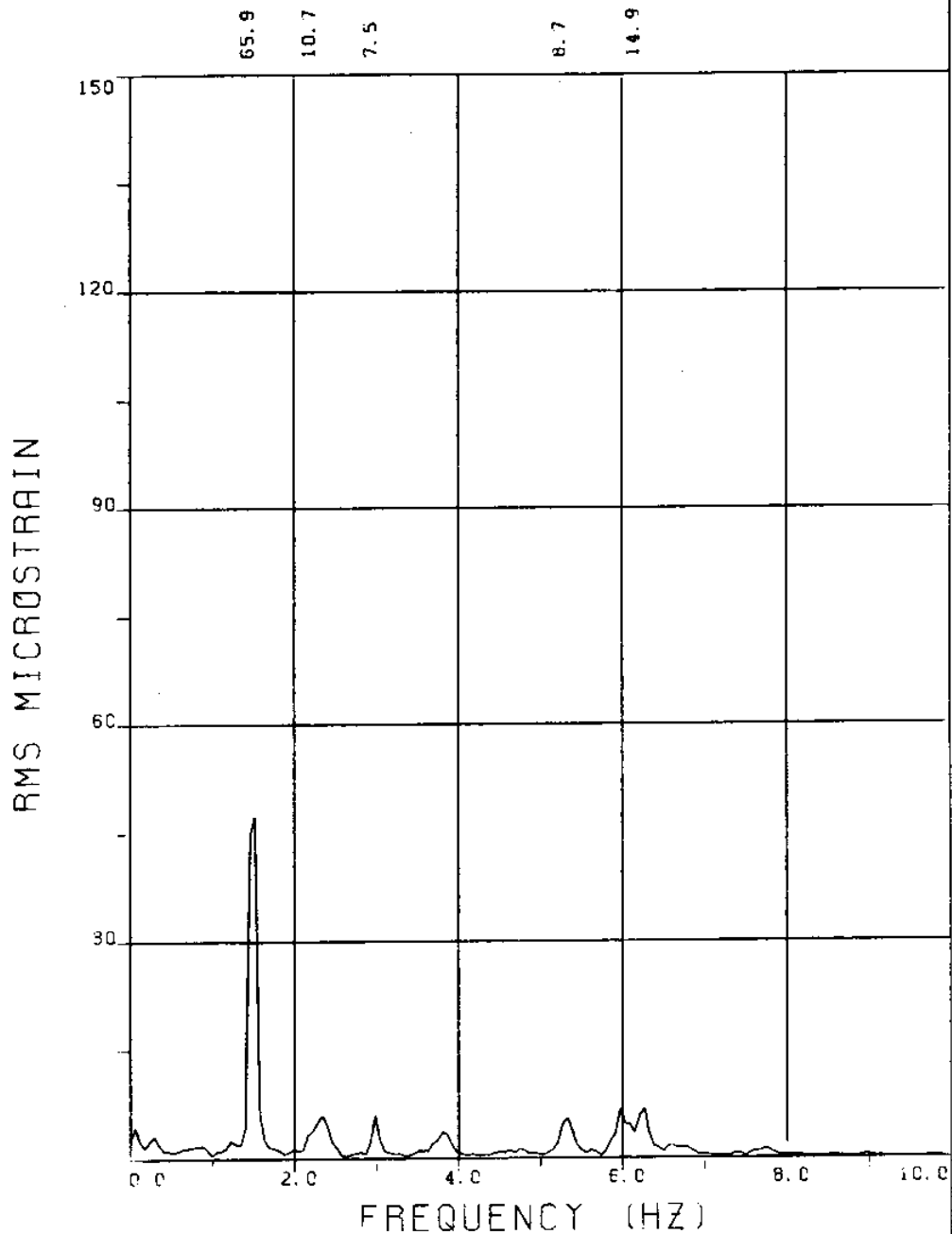


EXPERIMENT NUMBER 10

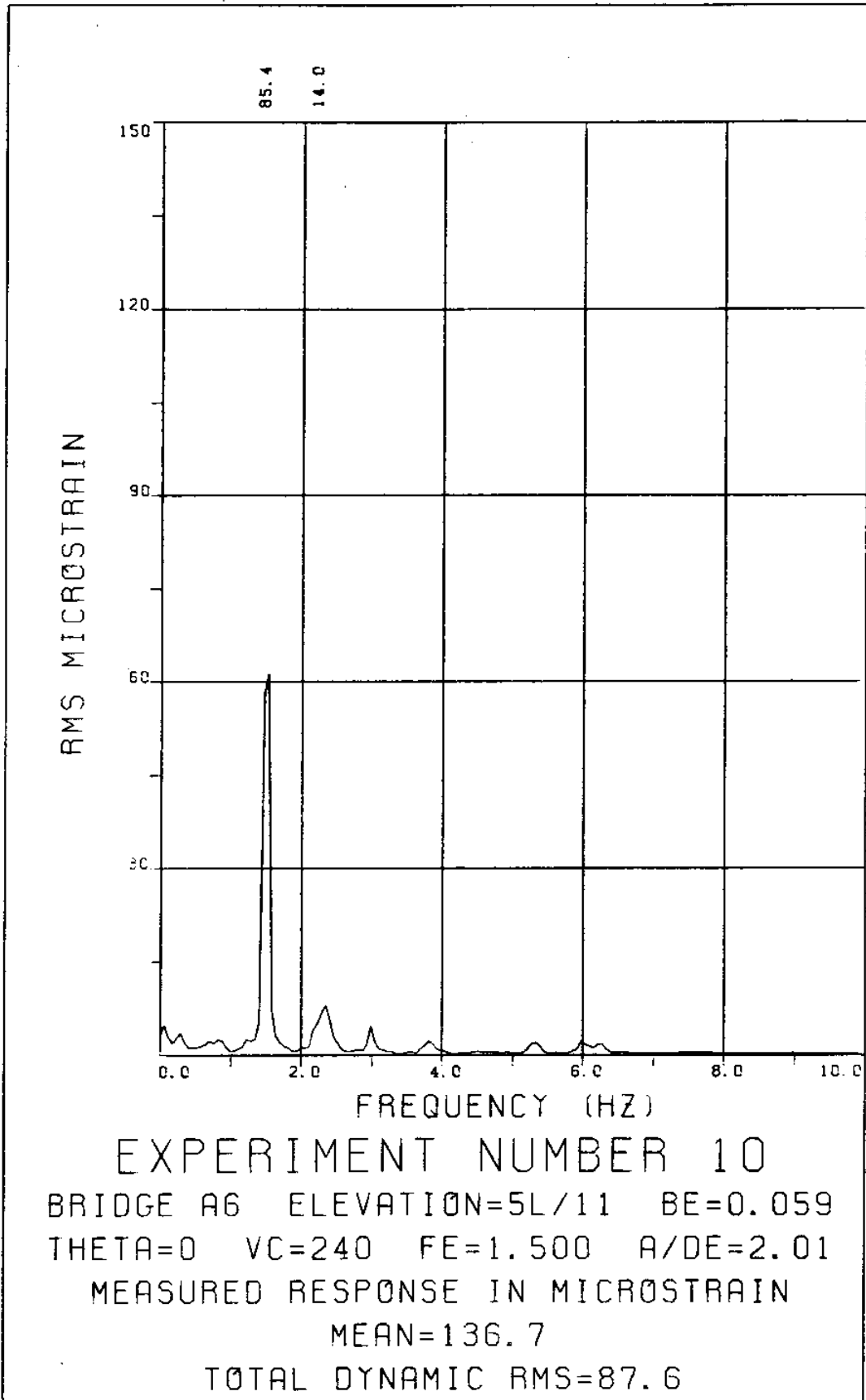
LVDT

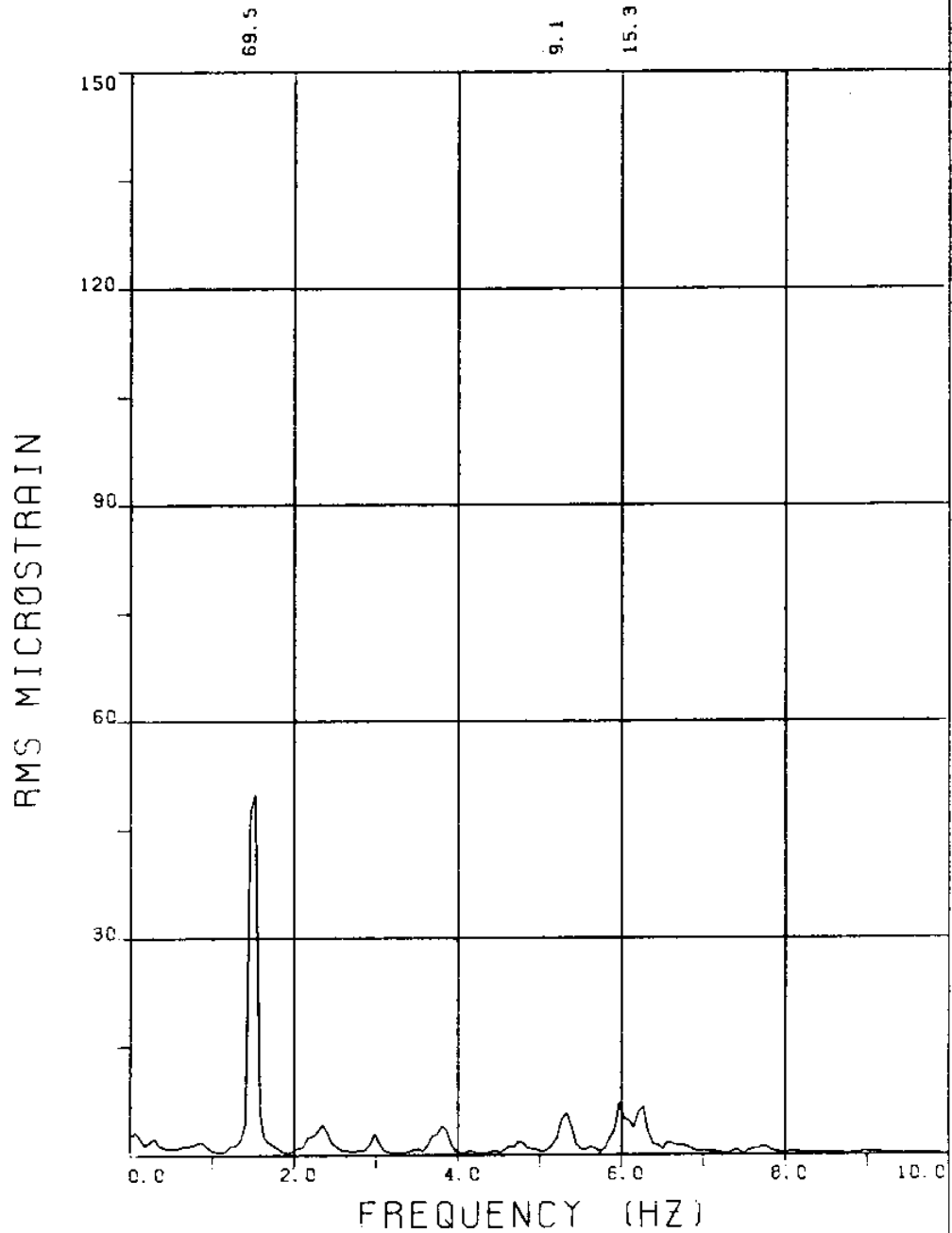
THETA=0 VC=240 FE=1.500 BE=0.059

MEASURED A/DE=2.01

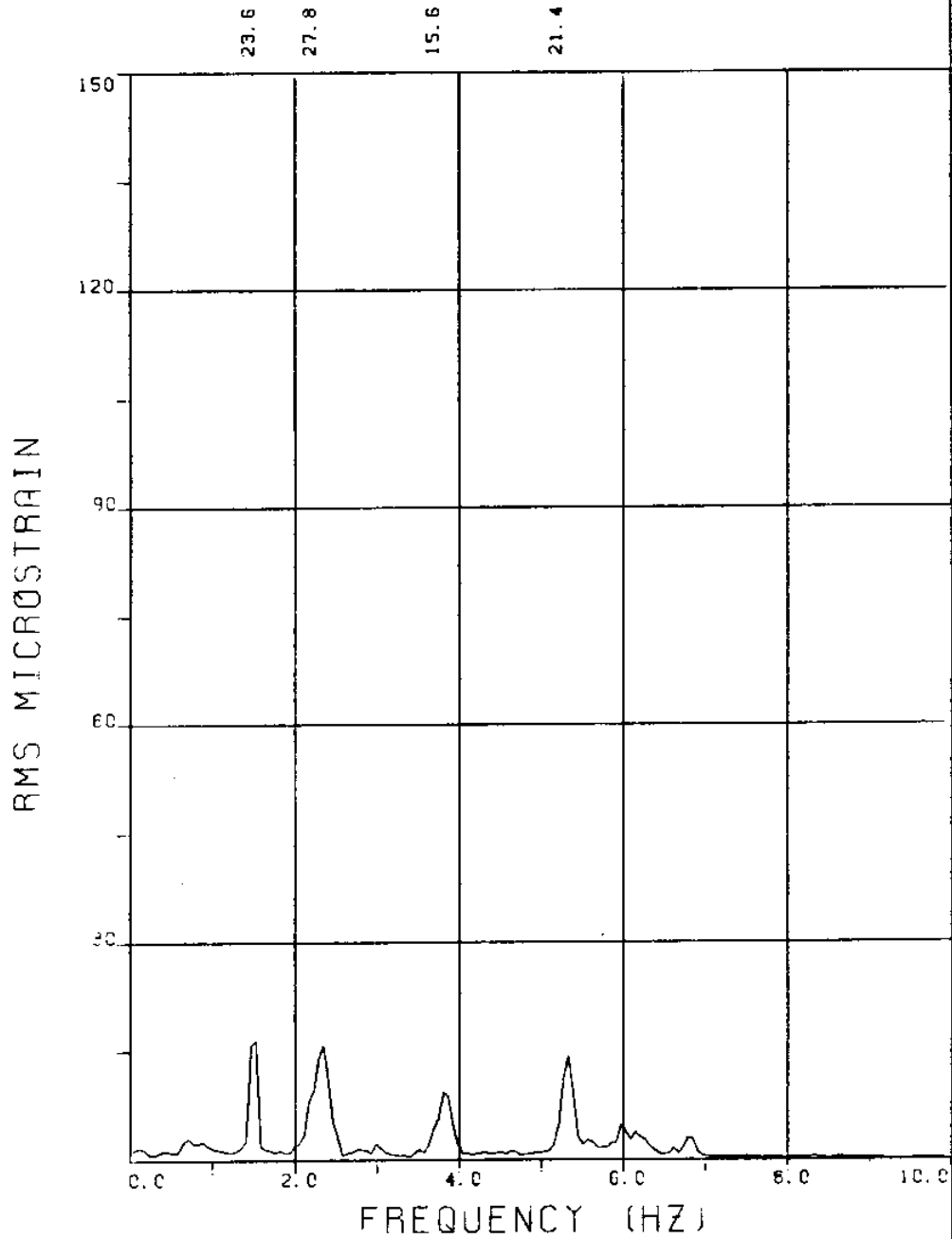


EXPERIMENT NUMBER 10
 BRIDGE A8 ELEVATION=3L/11 BE=0.059
 THETA=0 VC=240 FE=1.500 A/DE=2.01
 MEASURED RESPONSE IN MICROSTRAIN
 MEAN=112.0
 TOTAL DYNAMIC RMS=70.3





EXPERIMENT NUMBER 10
BRIDGE A3 ELEVATION=8L/11 BE=0.059
THETA=0 VC=240 FE=1.500 A/DE=2.01
MEASURED RESPONSE IN MICROSTRAIN
MEAN=115.7
TOTAL DYNAMIC RMS=73.1



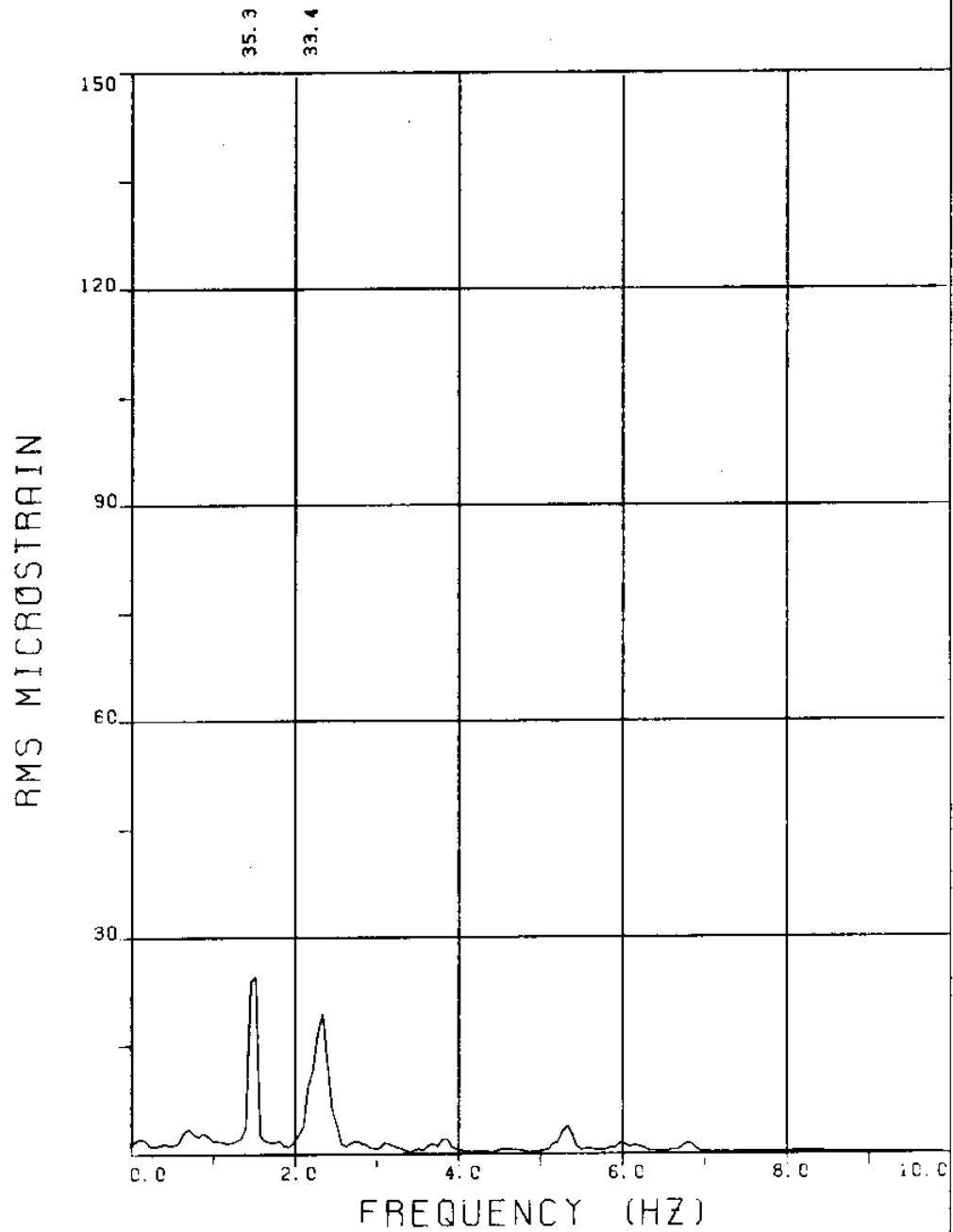
EXPERIMENT NUMBER 10

BRIDGE B8 ELEVATION=3L/11 BE=0.059

THETA=0 VC=240 FE=1.500 A/DE=2.01

MEASURED RESPONSE IN MICROSTRAIN

TOTAL DYNAMIC RMS=47.6



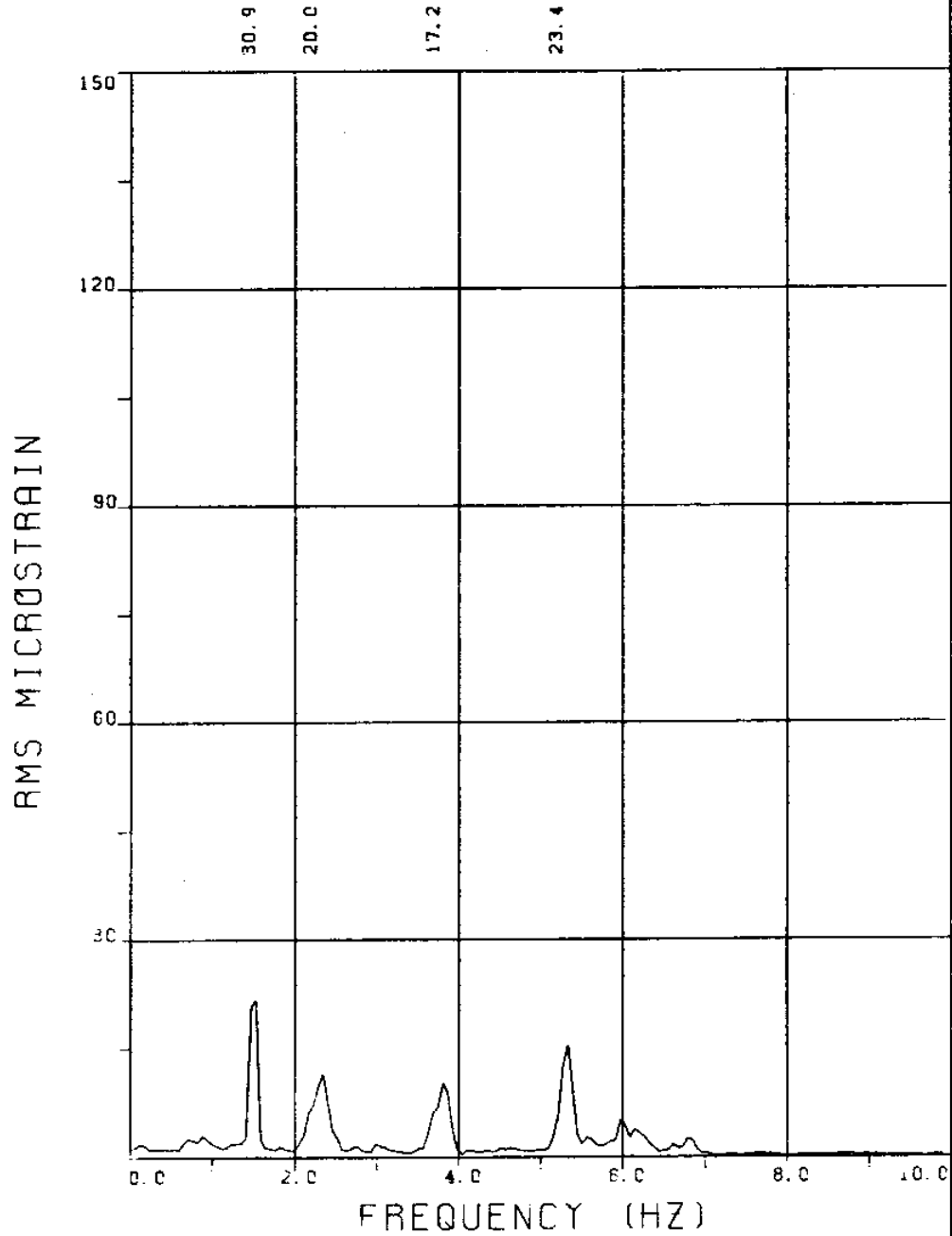
EXPERIMENT NUMBER 10

BRIDGE B5 ELEVATION=6L/11 BE=0.059

THETA=0 VC=240 FE=1.500 A/DE=2.01

MEASURED RESPONSE IN MICROSTRAIN

TOTAL DYNAMIC RMS=50.4



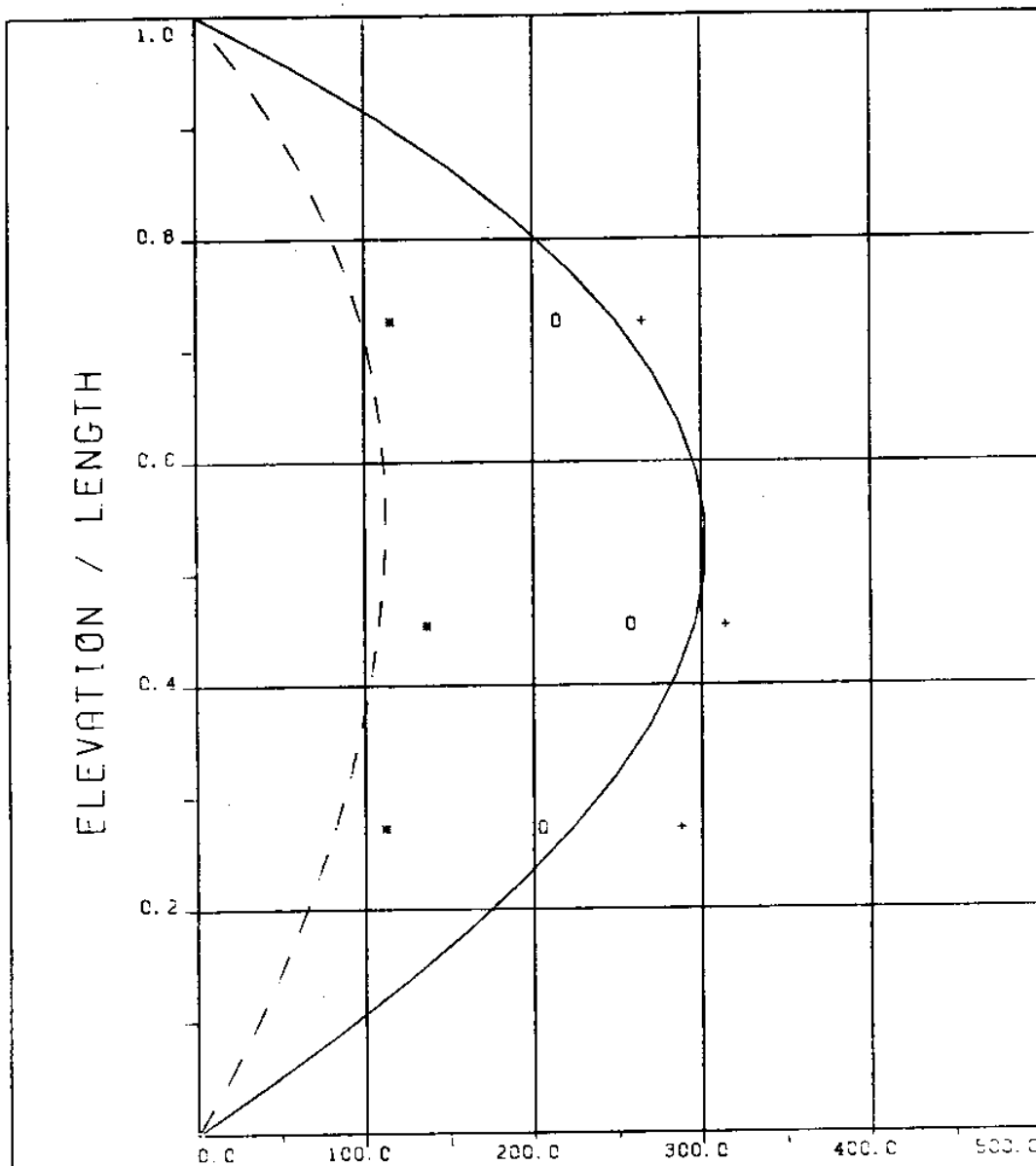
EXPERIMENT NUMBER 10

BRIDGE B3 ELEVATION=8L/11 BE=0.059

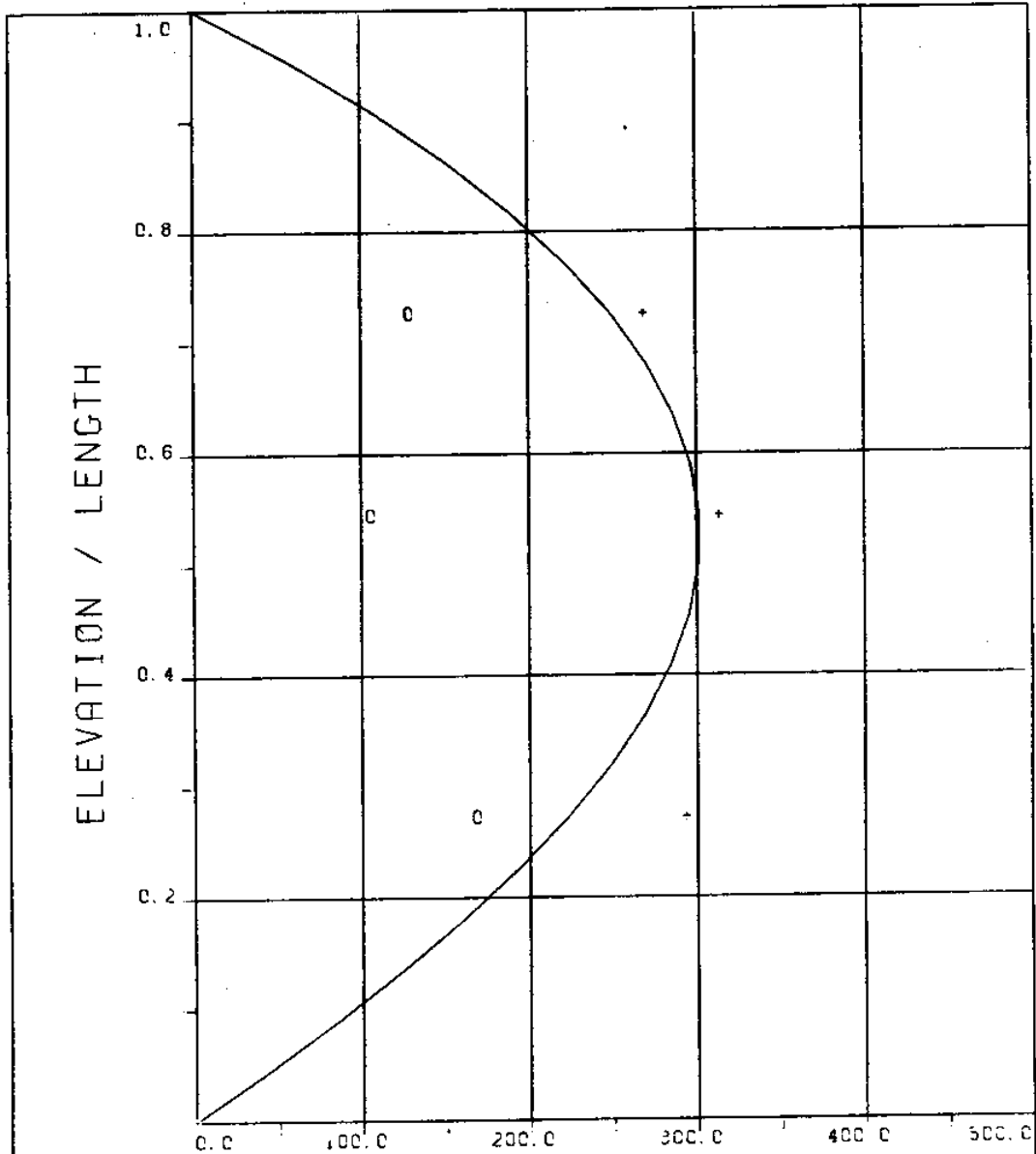
THETA=0 VC=240 FE=1.500 A/DE=2.01

MEASURED RESPONSE IN MICROSTRAIN

TOTAL DYNAMIC RMS=49.2



EXPERIMENT NUMBER 10
 THETA=0 VC=240 FE=1.500 A/DE=2.01
 STATIC RESPONSE IN PLANE A
 ----- THEORY * * * EXPERIMENT
 STATIC RESPONSE PLUS DYNAMIC
 RESPONSE AT F = FE IN PLANE A
 _____ THEORY o o o EXPERIMENT
 _____ THEORY + + + EXPERIMENT



EXPERIMENT NUMBER 10

THETA=0 VC=240 FE=1.500 A/DE=2.01

MAXIMUM DYNAMIC RESPONSE IN PLANE B

o o o EXPERIMENT

MAXIMUM RESPONSE

_____ THEORY + + + EXPERIMENT

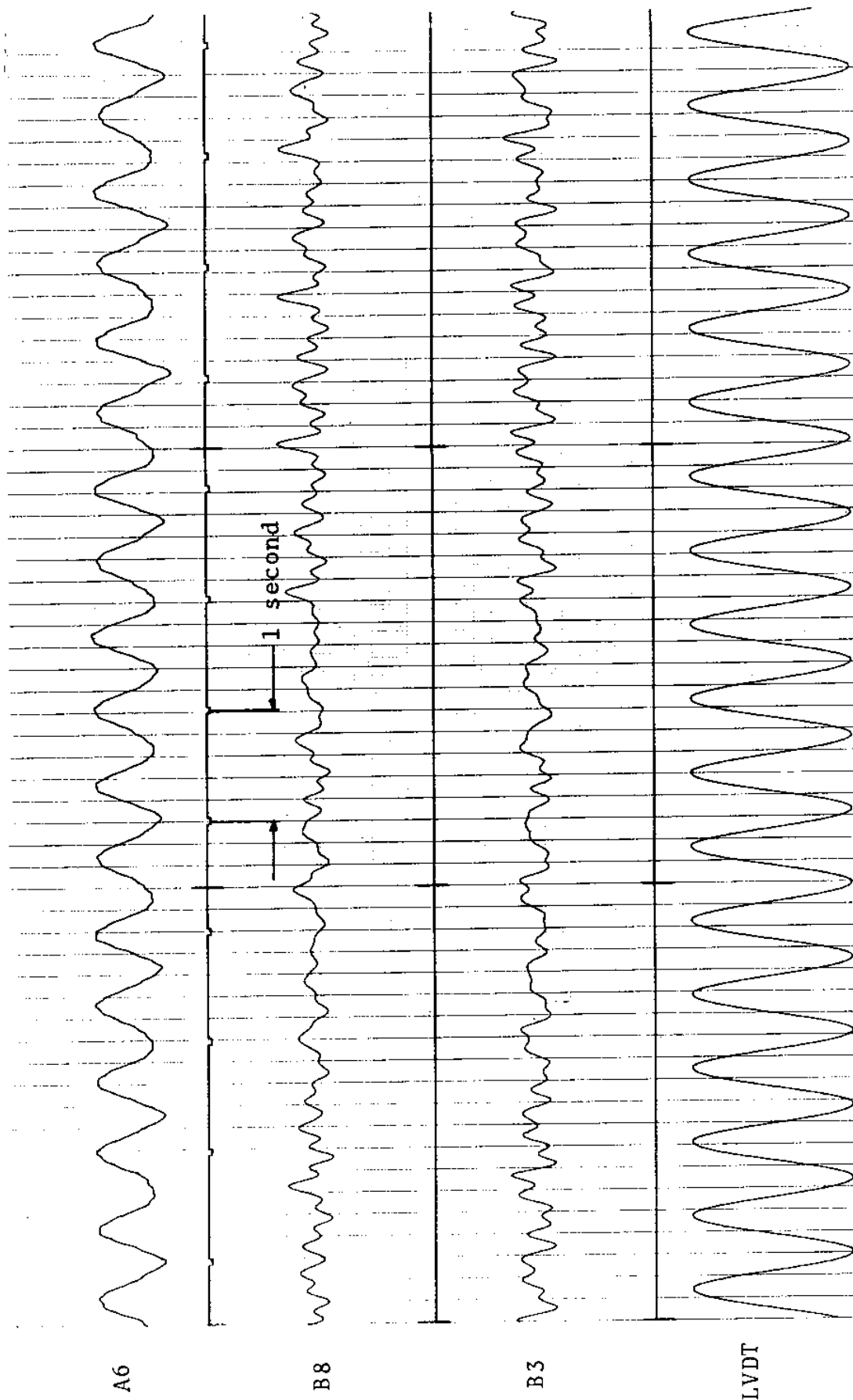


FIGURE 10Ta: LVDT: 0.087 D_e/DIVISION; STRAINS: 15.3 MICROSTRAIN/DIVISION

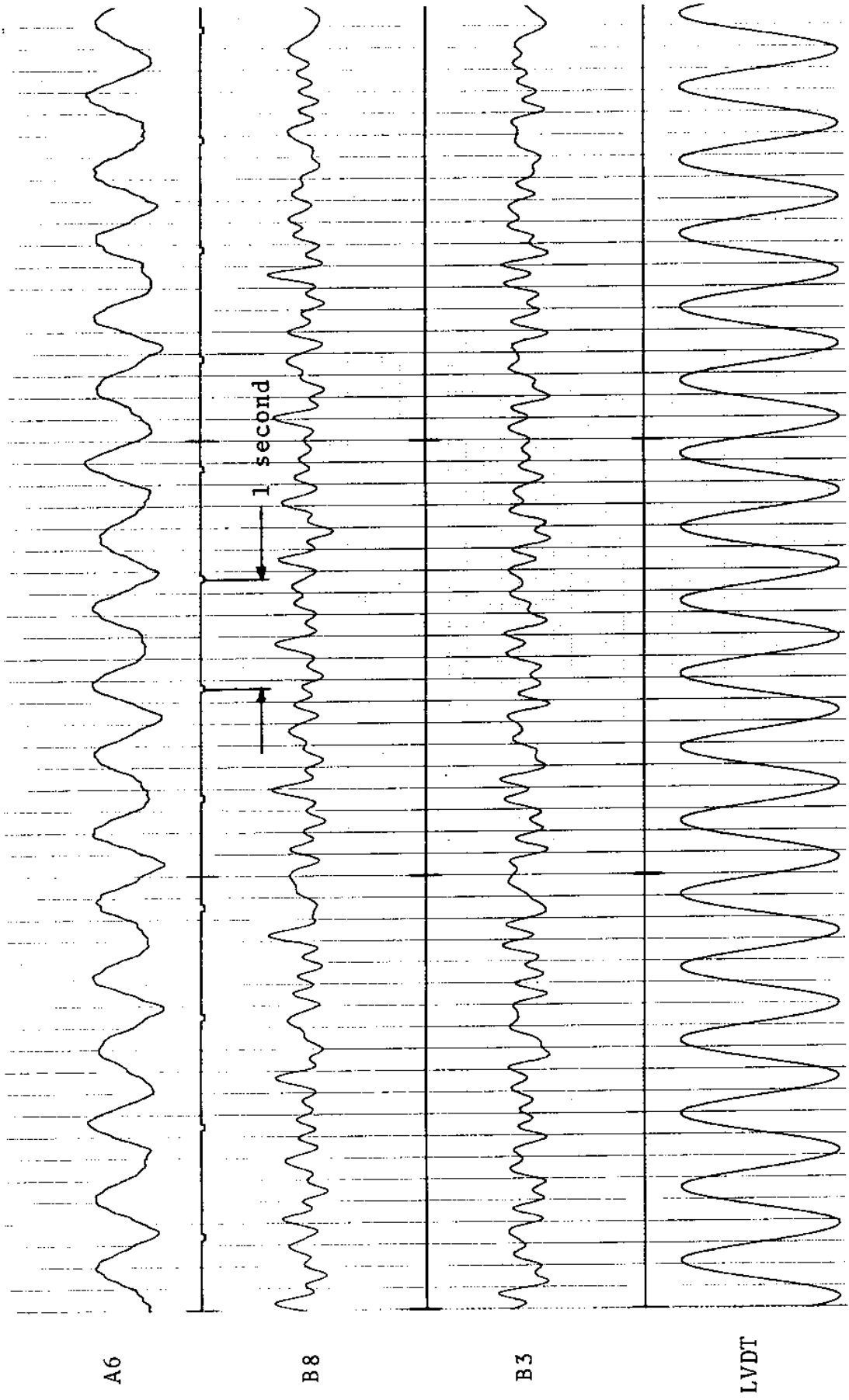
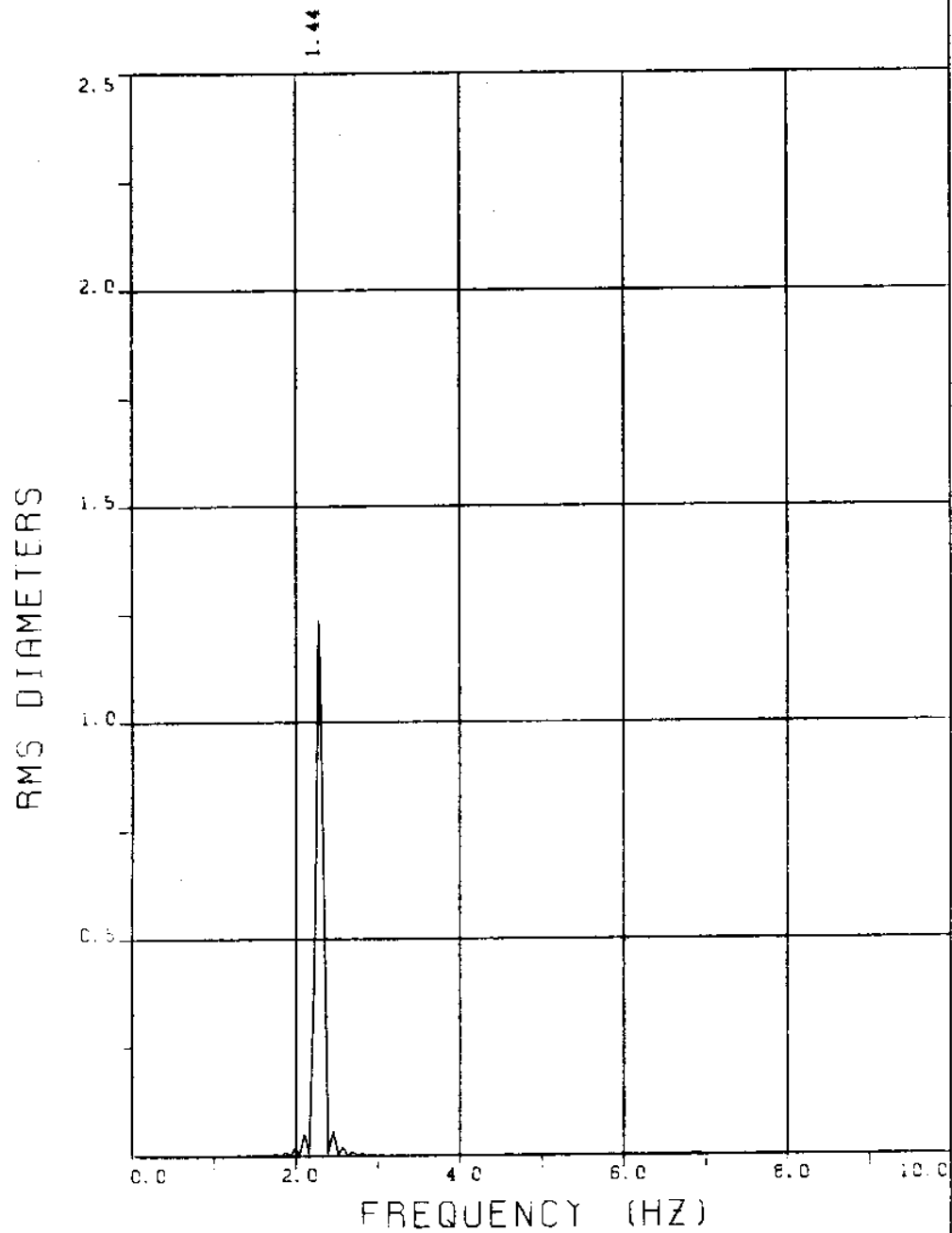


FIGURE 10Tb: LVDT: 0.087 D_e/DIVISION; STRAINS: 15.3 MICROSTRAIN/DIVISION

EXPERIMENT 8

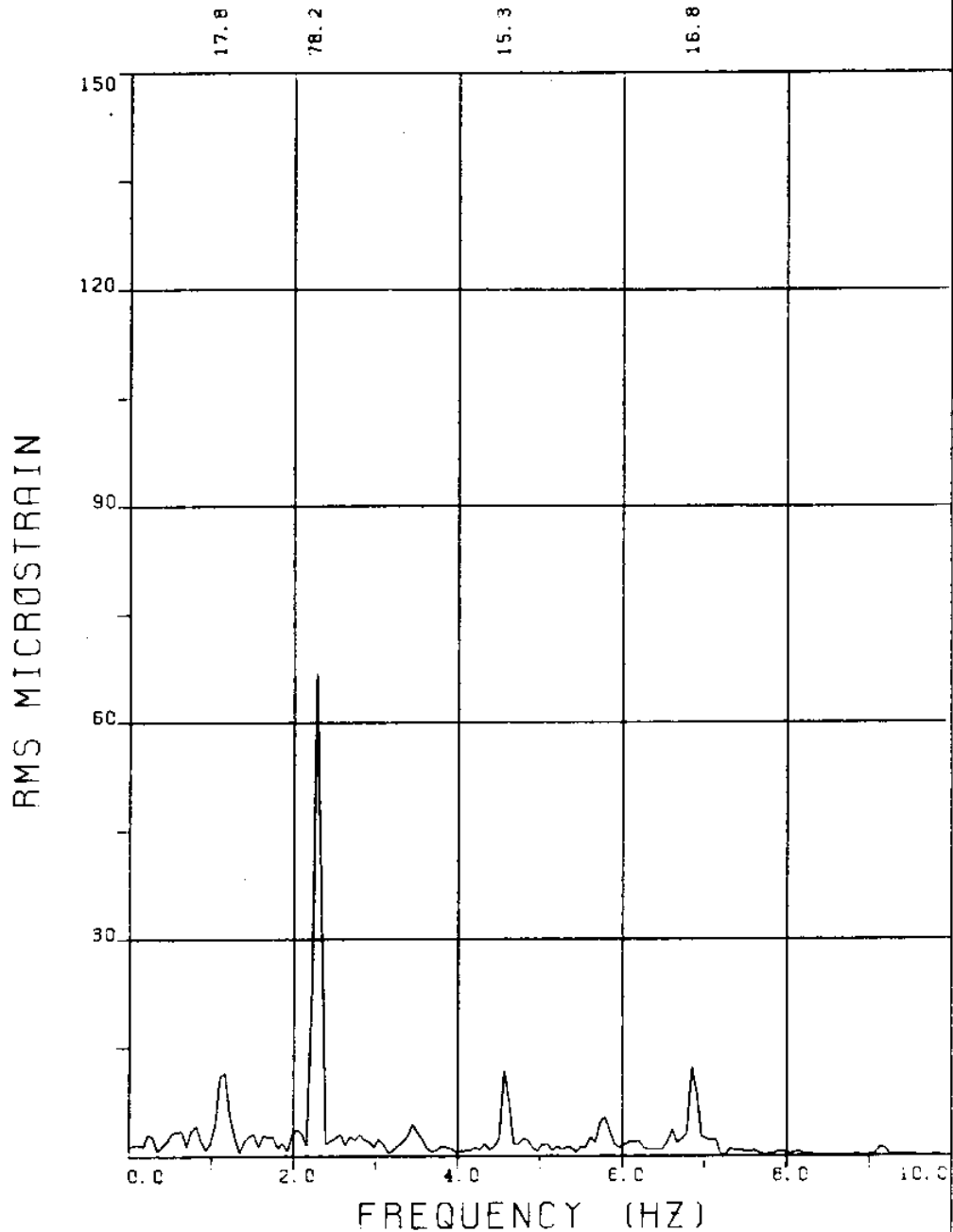


EXPERIMENT NUMBER 8

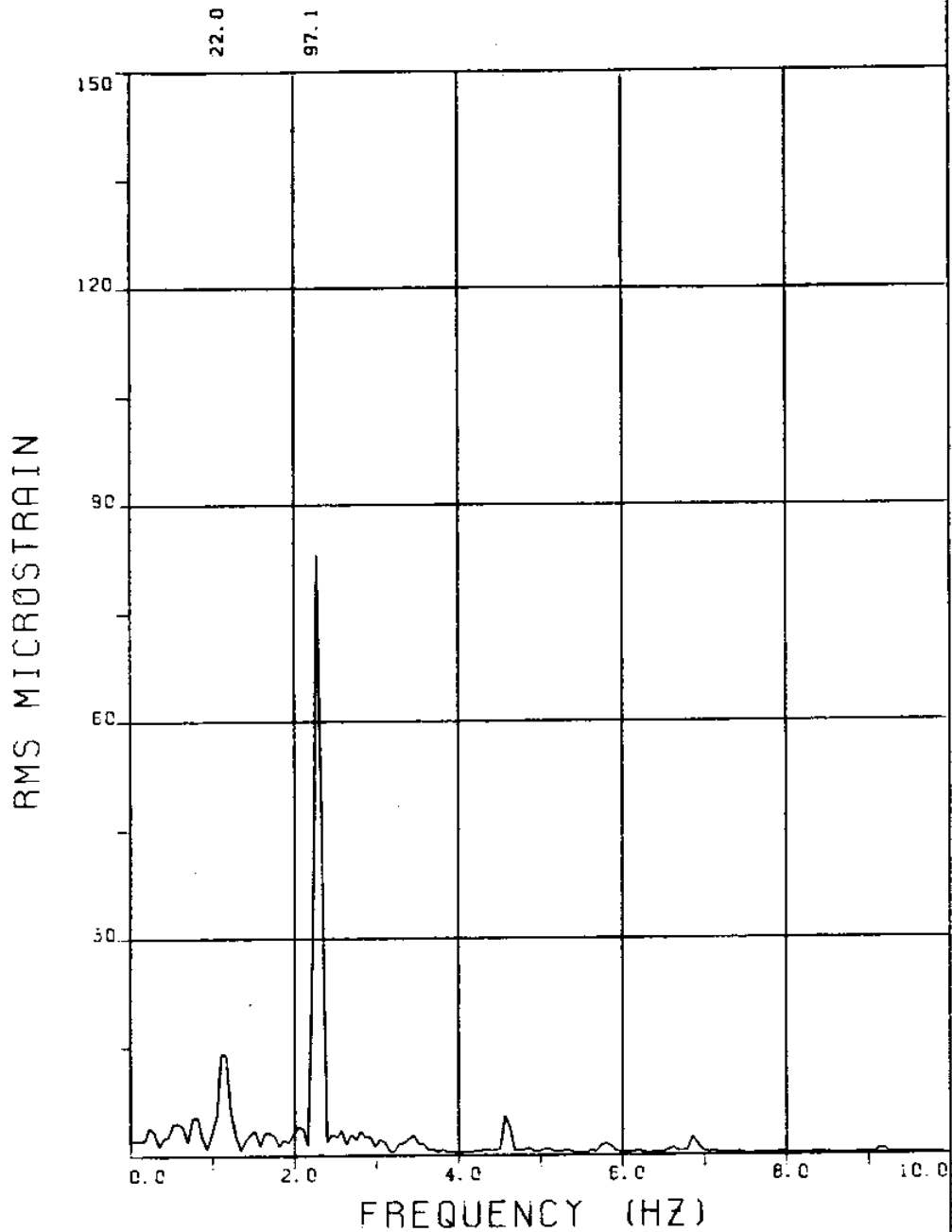
LVDT

THETA=0 VC=240 FE=2.300 BE=0.059

MEASURED A/DE=2.04



EXPERIMENT NUMBER 8
 BRIDGE A8 ELEVATION=3L/11 BE=0.059
 THETA=0 VC=240 FE=2.300 A/DE=2.04
 MEASURED RESPONSE IN MICROSTRAIN
 MEAN=118.2
 TOTAL DYNAMIC RMS=85.4



EXPERIMENT NUMBER 8

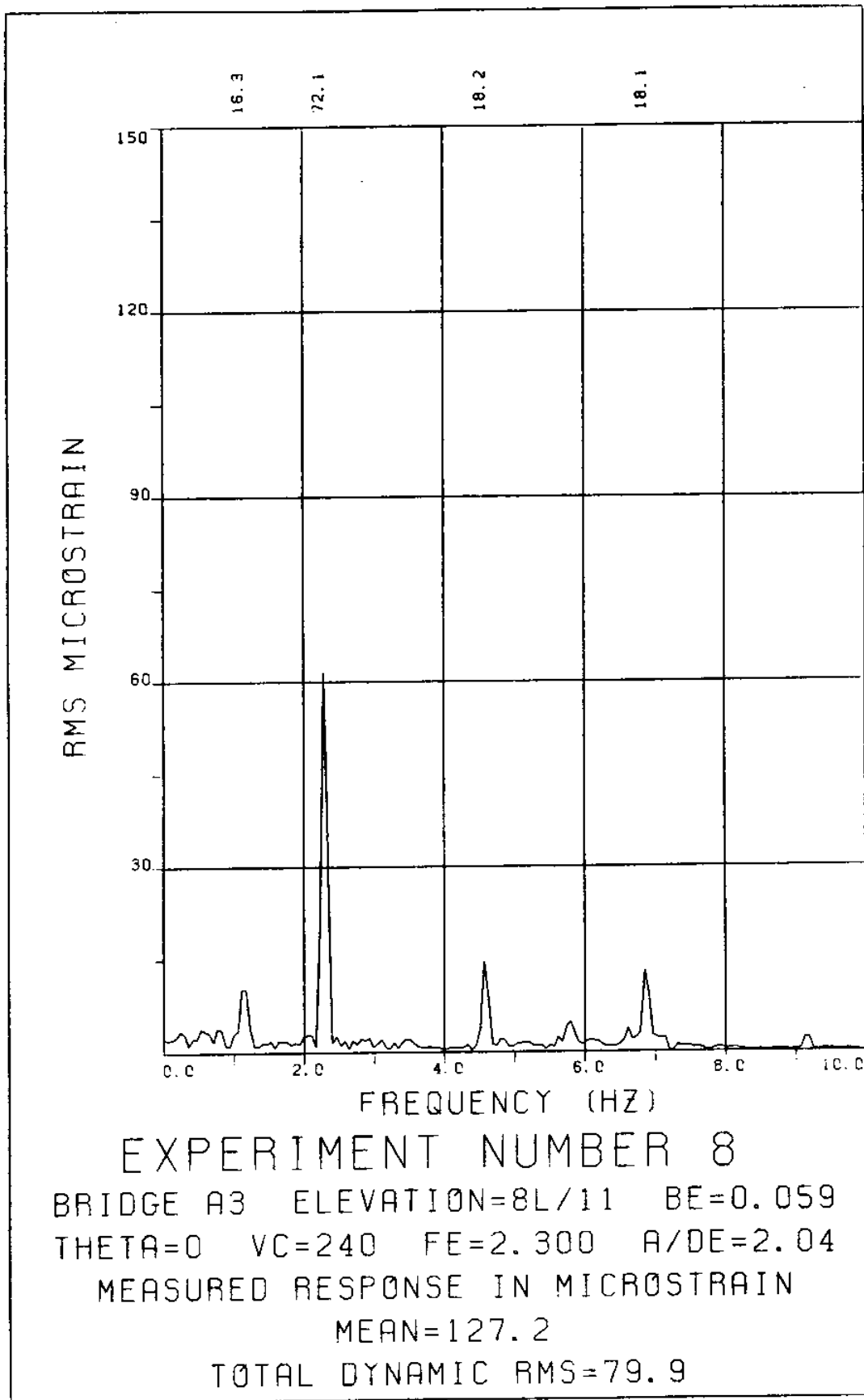
BRIDGE A6 ELEVATION=5L/11 BE=0.059

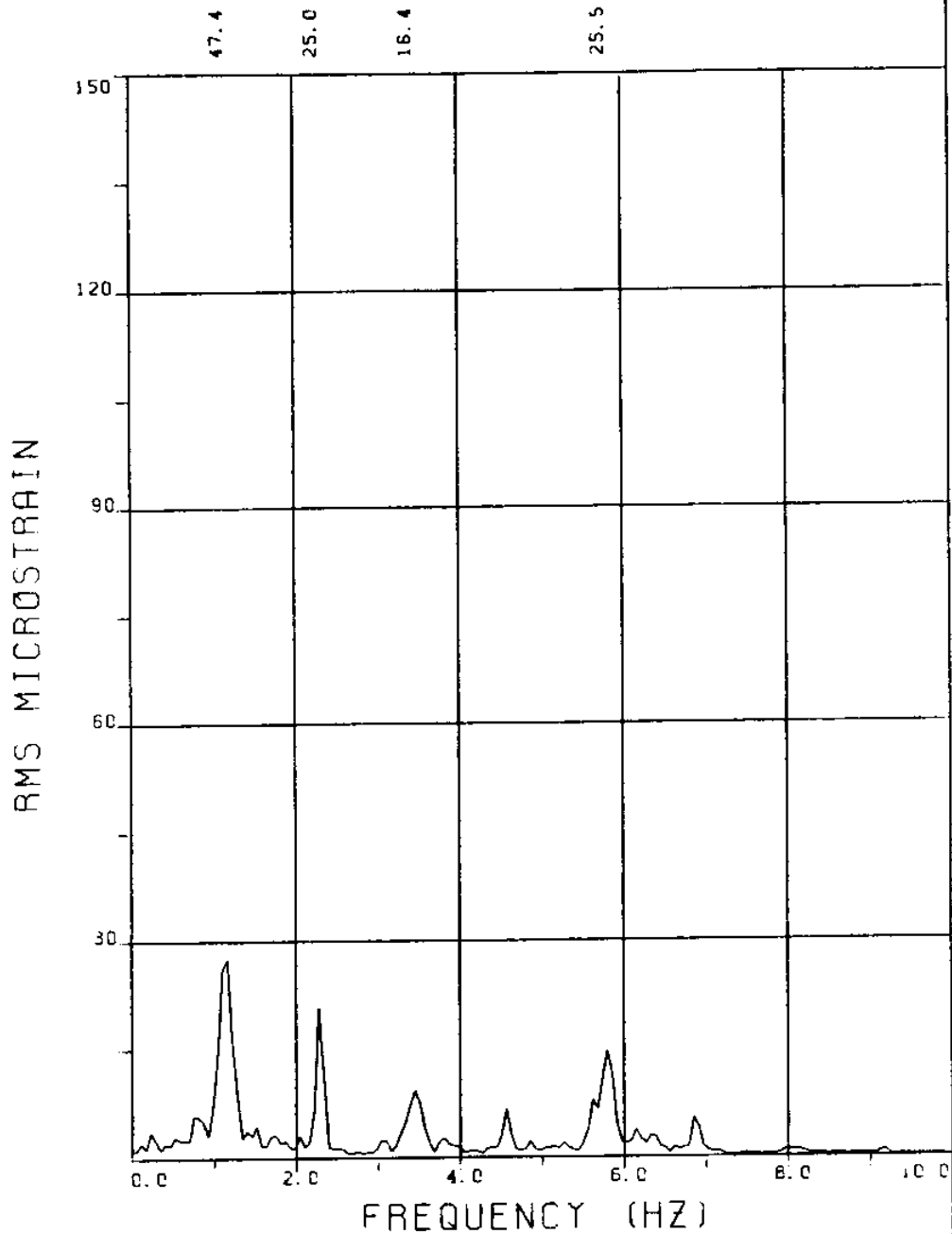
THETA=0 VC=240 FE=2.300 A/DE=2.04

MEASURED RESPONSE IN MICROSTRAIN

MEAN=143.4

TOTAL DYNAMIC RMS=101.5





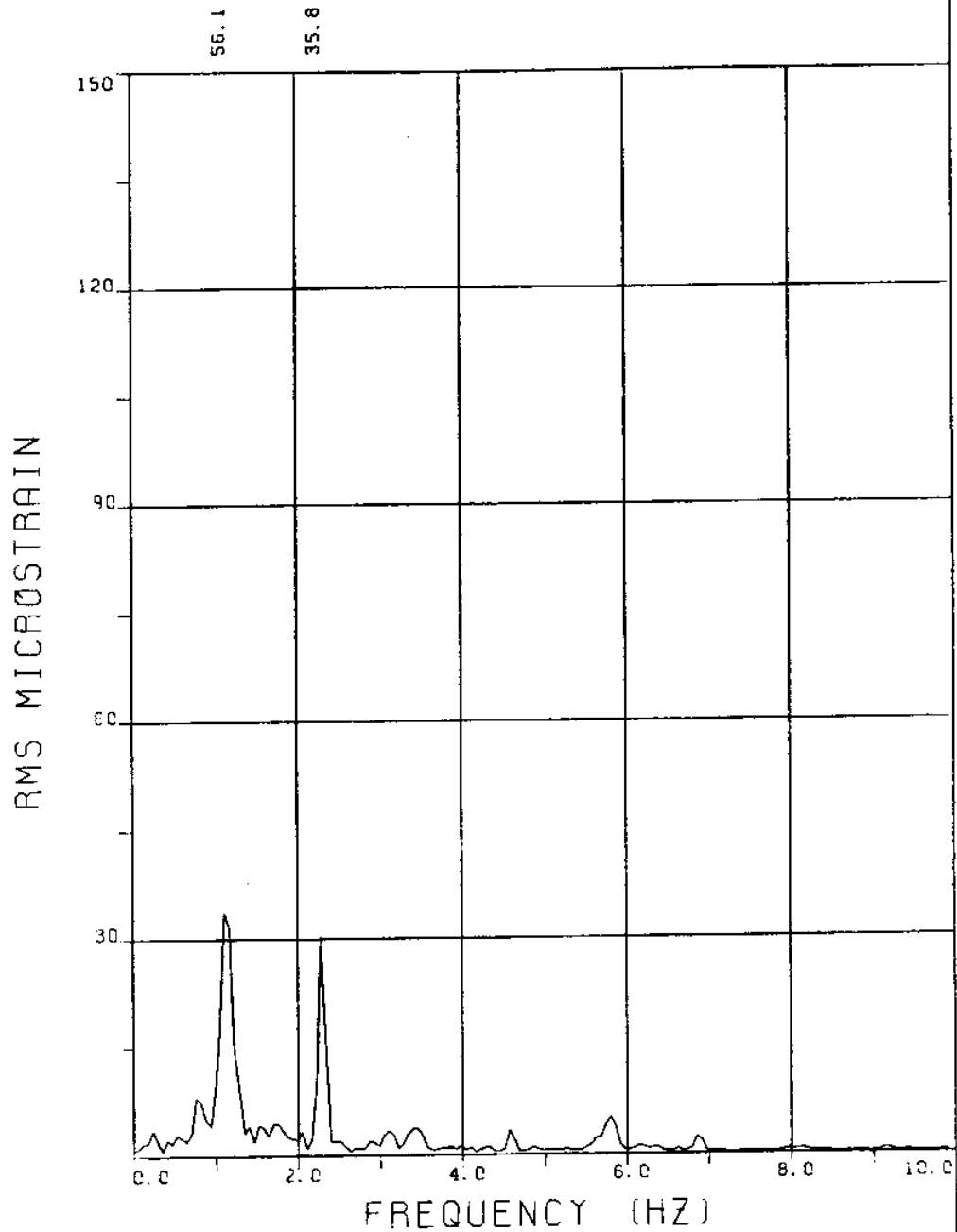
EXPERIMENT NUMBER 8

BRIDGE B8 ELEVATION=3L/11 BE=0.059

THETA=0 VC=240 FE=2.300 A/DE=2.04

MEASURED RESPONSE IN MICROSTRAIN

TOTAL DYNAMIC RMS=63.4



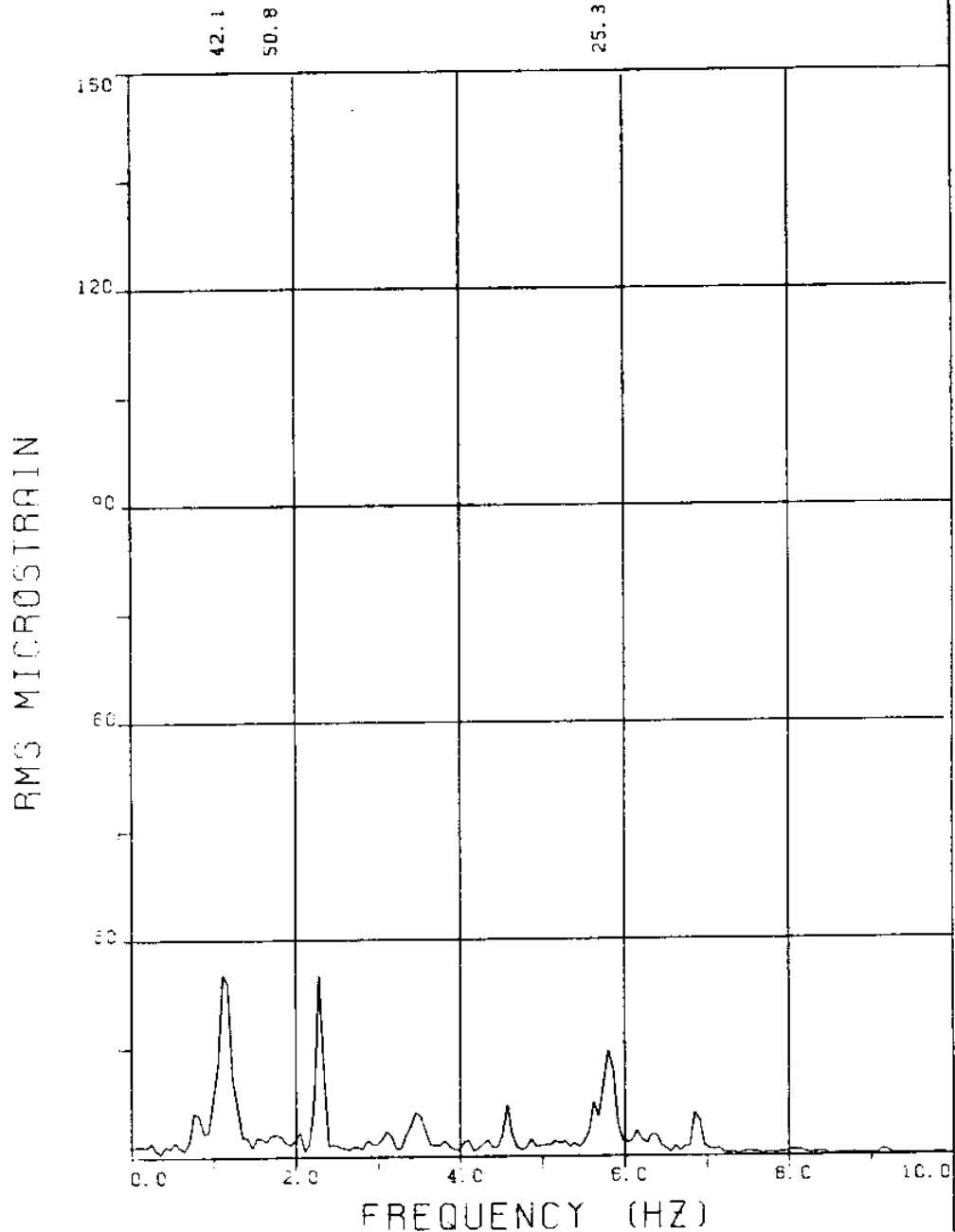
EXPERIMENT NUMBER 8

BRIDGE B5 ELEVATION=6L/11 BE=0.059

THETA=0 VC=240 FE=2.300 A/DE=2.04

MEASURED RESPONSE IN MICROSTRAIN

TOTAL DYNAMIC RMS=68.5



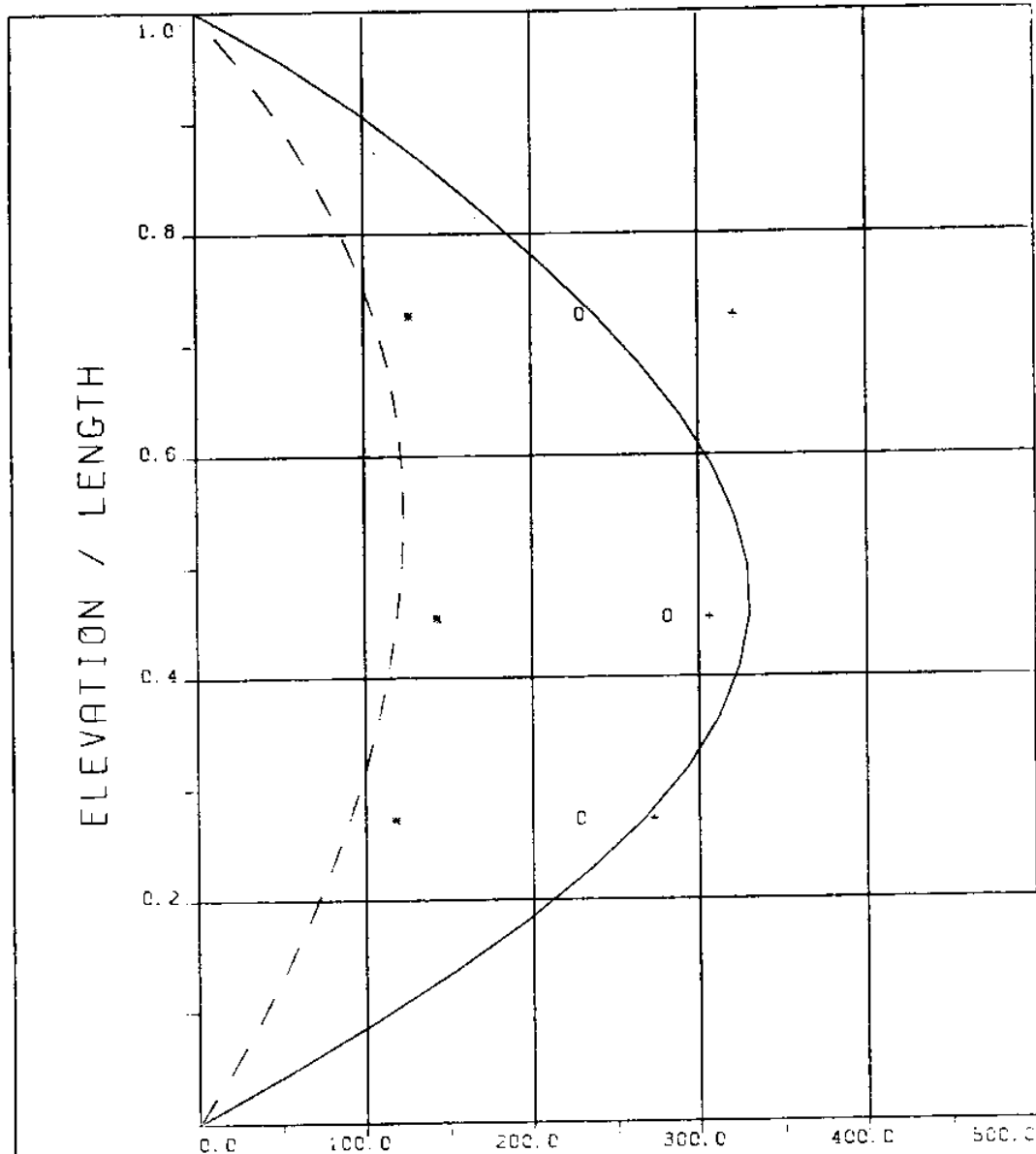
EXPERIMENT NUMBER 8

BRIDGE B3 ELEVATION=8L/11 BE=0.059

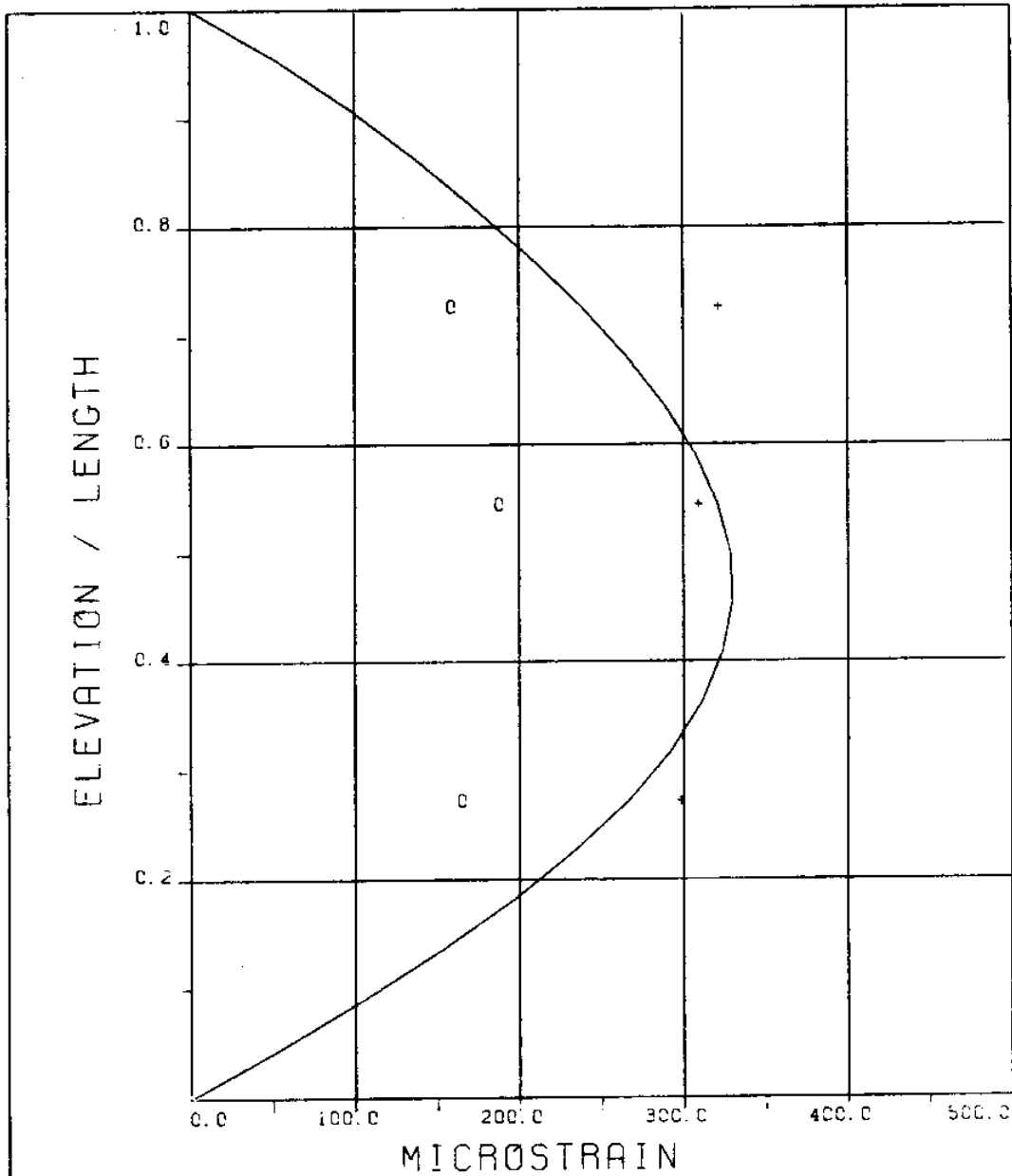
THETA=0 VC=240 FE=2.300 A/DE=2.04

MEASURED RESPONSE IN MICROSTRAIN

TOTAL DYNAMIC RMS=60.6



EXPERIMENT NUMBER 8
 THETA=0 VC=240 FE=2.300 A/DE=2.04
 STATIC RESPONSE IN PLANE A
 ----- THEORY * * * EXPERIMENT
 STATIC RESPONSE PLUS DYNAMIC
 RESPONSE AT $F = F_E$ IN PLANE A
 _____ THEORY o o o EXPERIMENT
 _____ THEORY + + + EXPERIMENT



EXPERIMENT NUMBER 8
 THETA=0 VC=240 FE=2.300 A/DE=2.04

MAXIMUM DYNAMIC RESPONSE IN PLANE B
 o o o EXPERIMENT

MAXIMUM RESPONSE
 _____ THEORY + + + EXPERIMENT

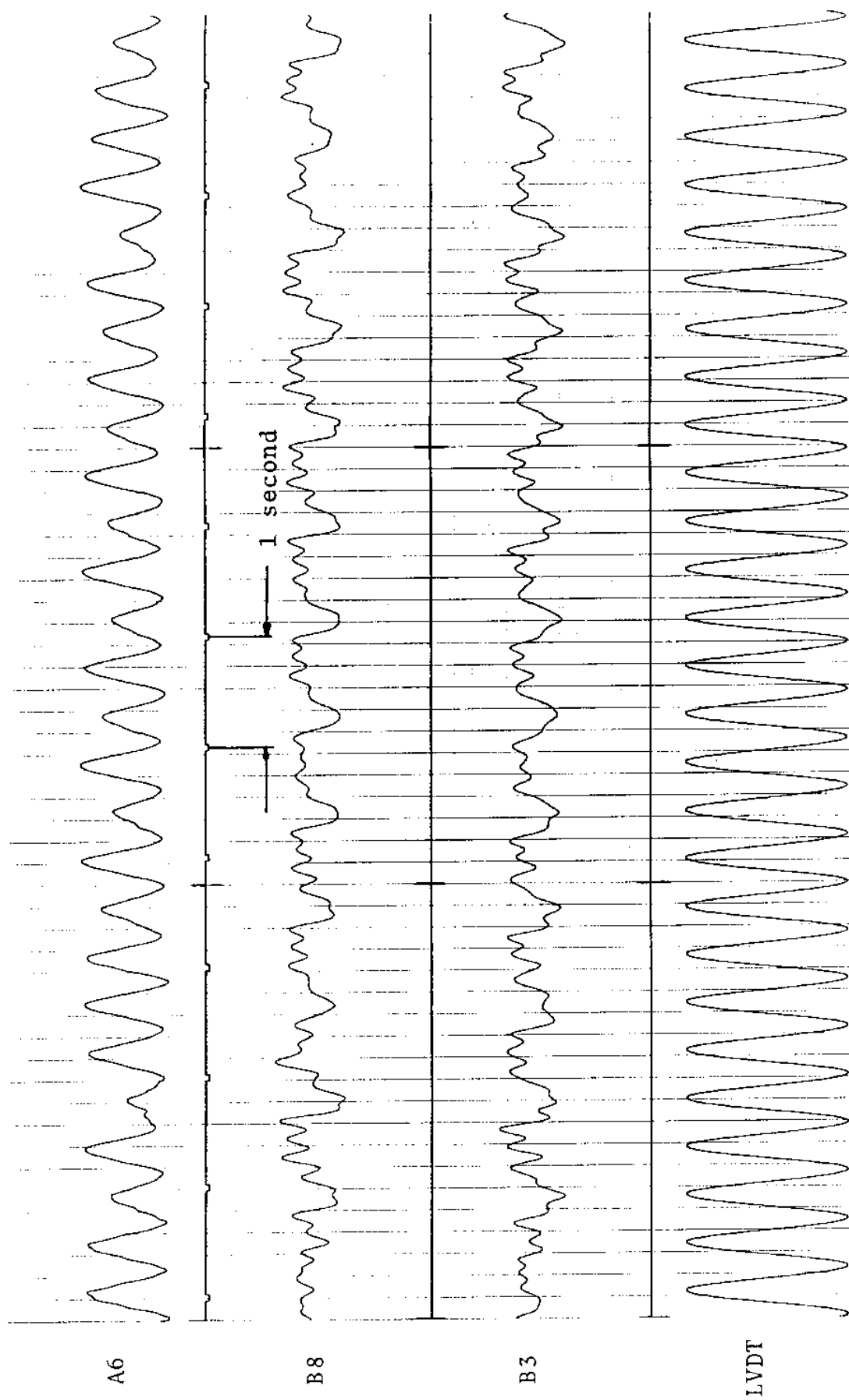


FIGURE 8Ta: LVDT: 0.087 D_e/DIVISION; STRAINS: 15.3 MICROSTRAIN/DIVISION

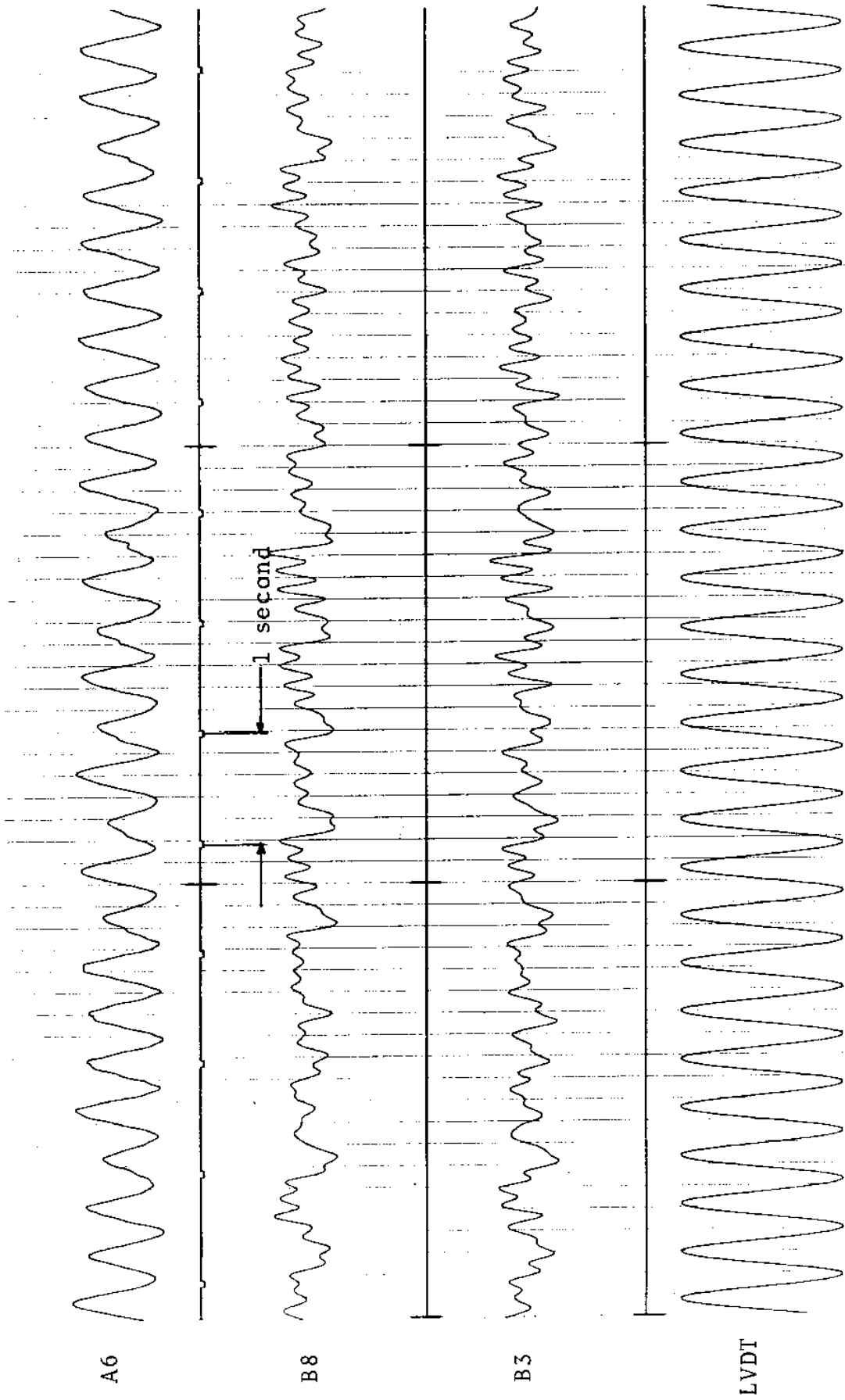
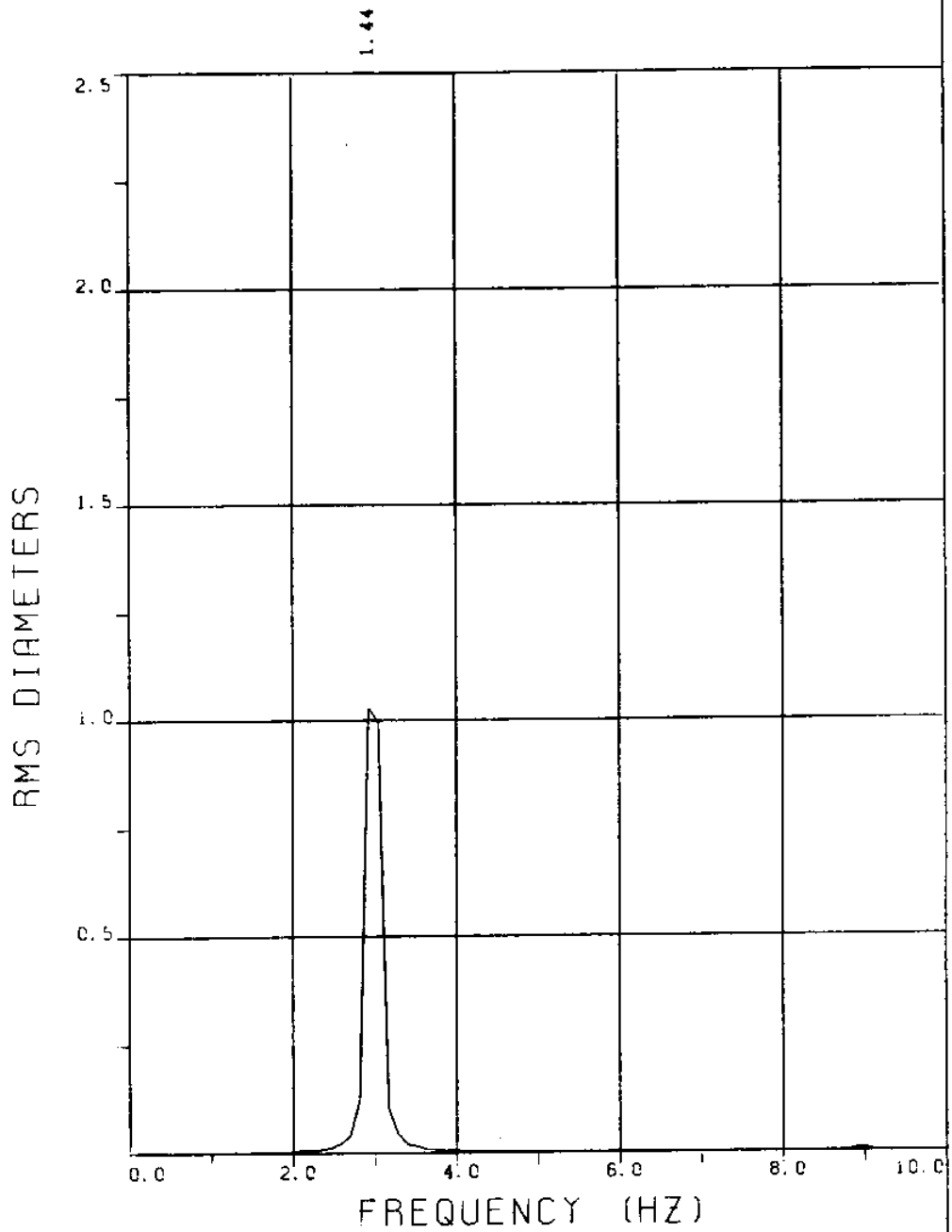


FIGURE 8Tb: LVDT: 0.087 D_e/DIVISION; STRAINS: 15.3 MICROSTRAIN/DIVISION

EXPERIMENT 7

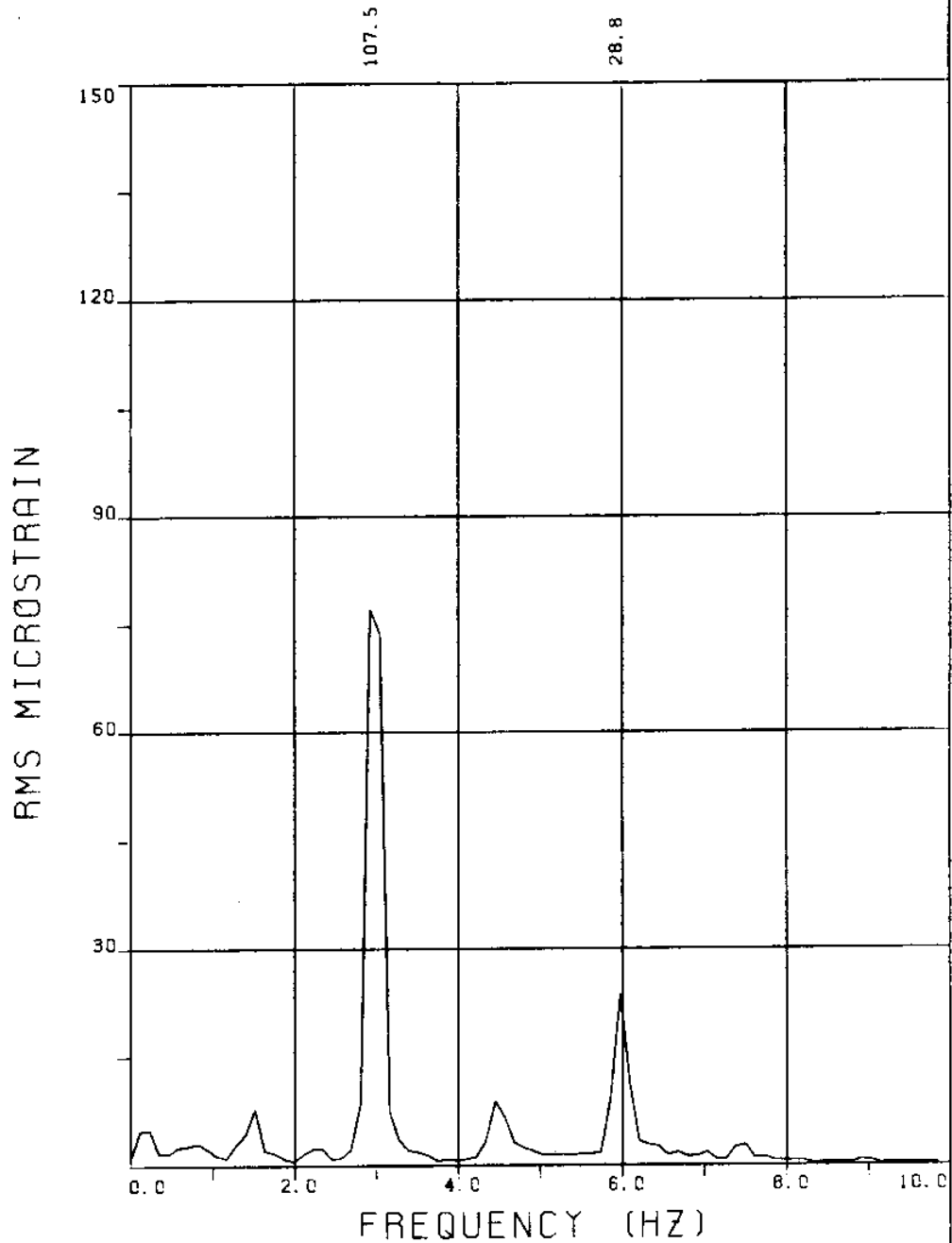


EXPERIMENT NUMBER 7

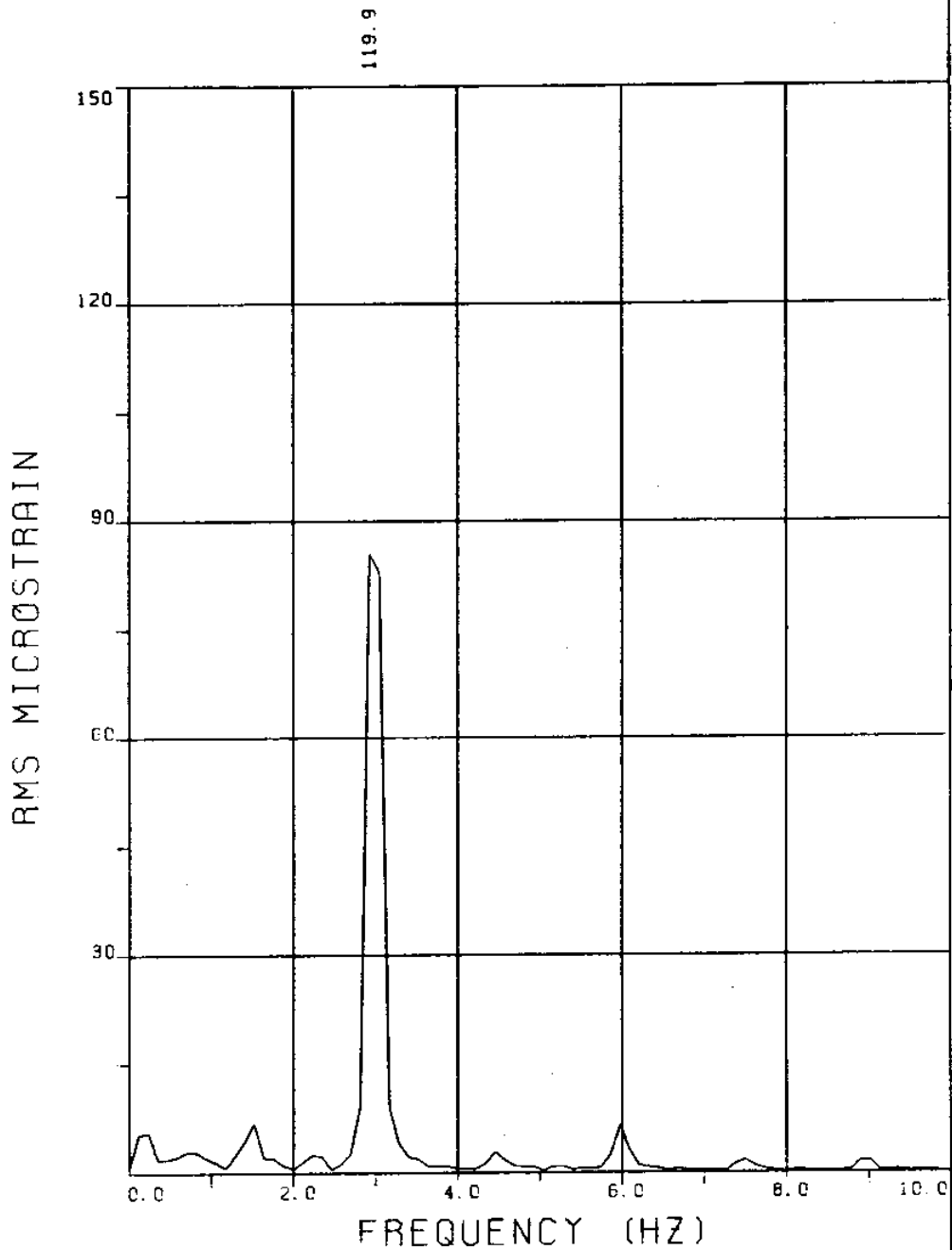
LVDT

THETA=0 VC=240 FE=3.000 BE=0.117

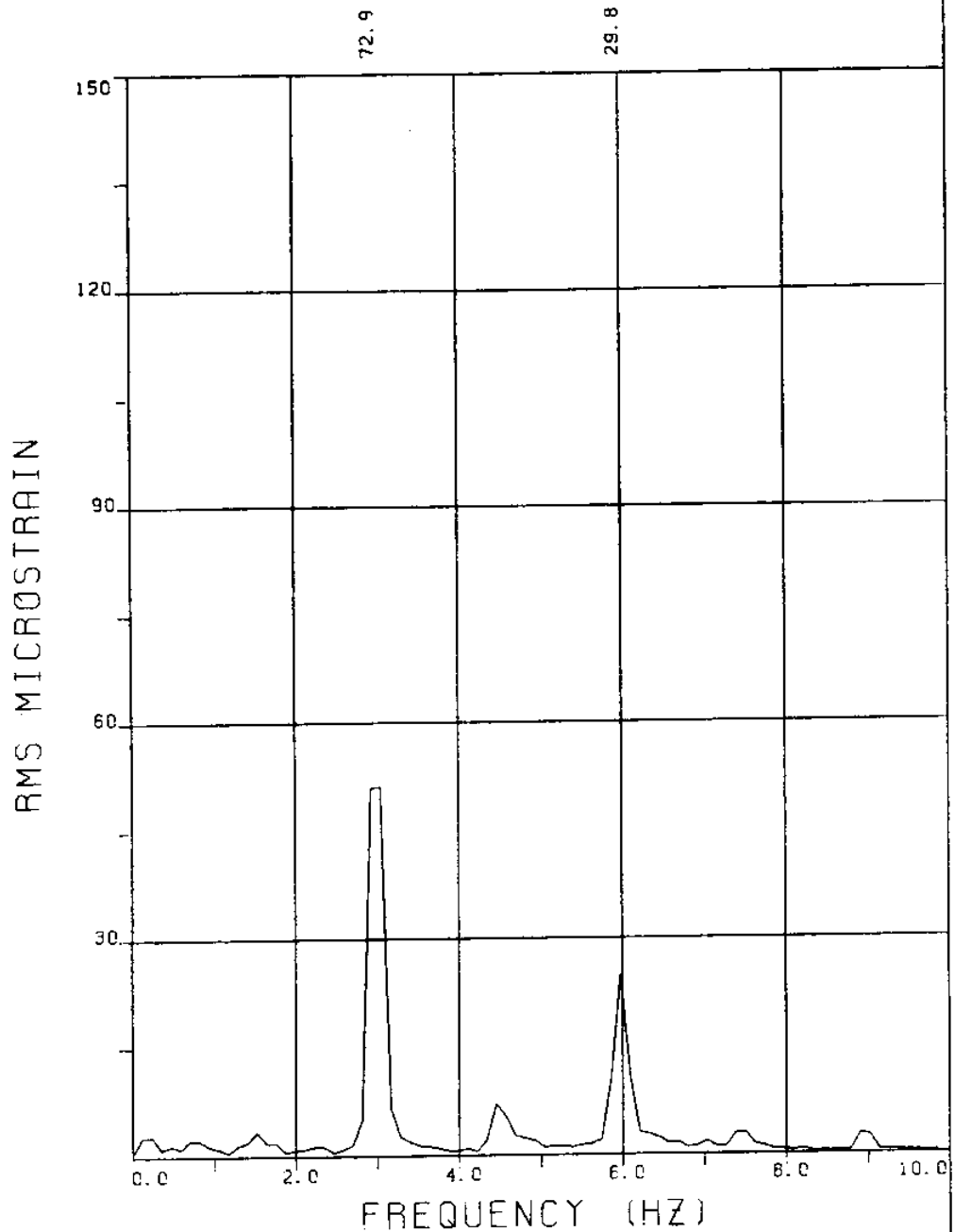
MEASURED A/DE=2.04



EXPERIMENT NUMBER 7
BRIDGE A8 ELEVATION=3L/11 BE=0.117
THETA=0 VC=240 FE=3.000 A/DE=2.04
MEASURED RESPONSE IN MICROSTRAIN
MEAN=116.9
TOTAL DYNAMIC RMS=112.9



EXPERIMENT NUMBER 7
 BRIDGE A6 ELEVATION=5L/11 BE=0.117
 THETA=0 VC=240 FE=3.000 A/DE=2.04
 MEASURED RESPONSE IN MICROSTRAIN
 MEAN=141.2
 TOTAL DYNAMIC RMS=121.1



EXPERIMENT NUMBER 7

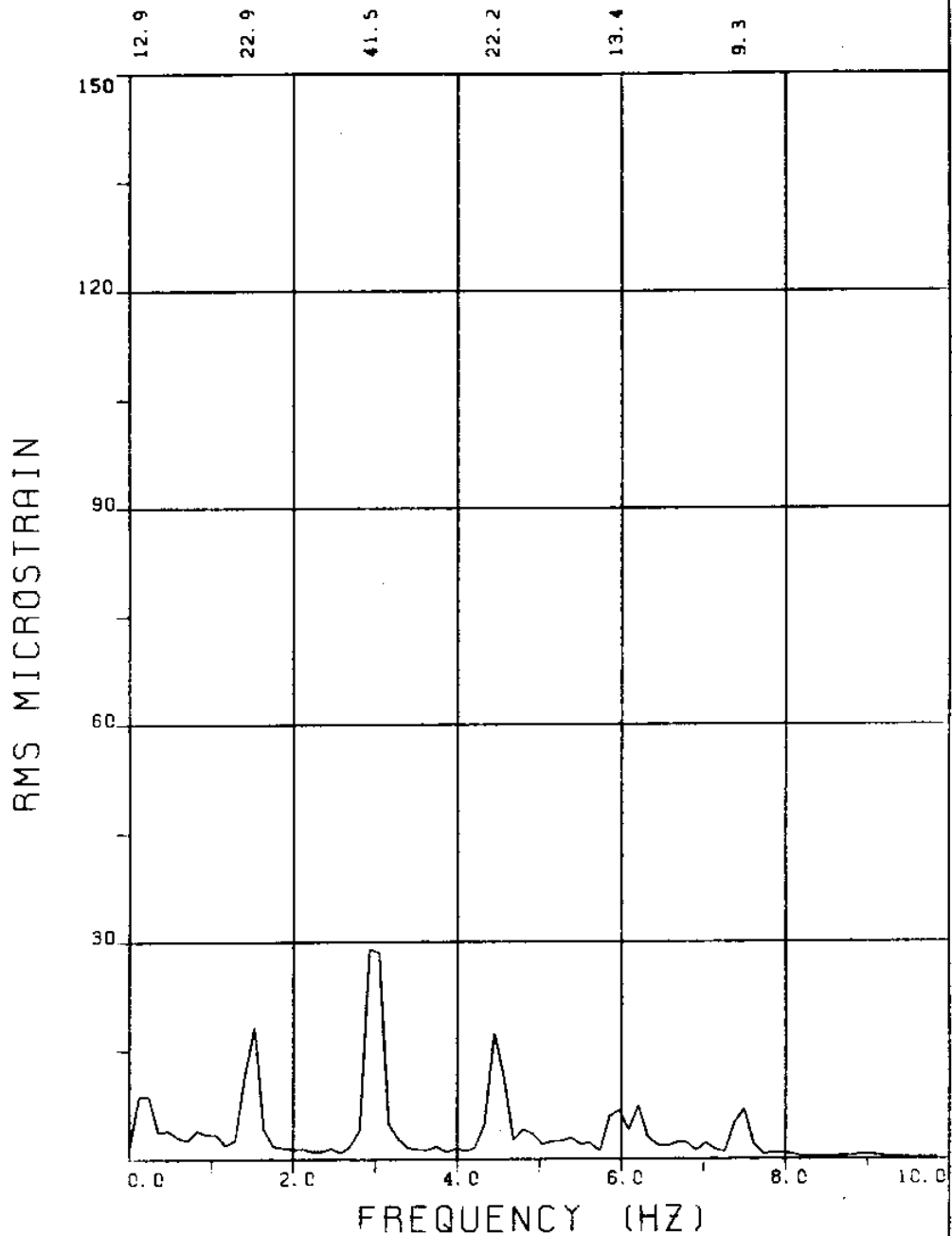
BRIDGE A3 ELEVATION=8L/11 BE=0.117

THETA=0 VC=240 FE=3.000 A/DE=2.04

MEASURED RESPONSE IN MICROSTRAIN

MEAN=121.7

TOTAL DYNAMIC RMS=80.0



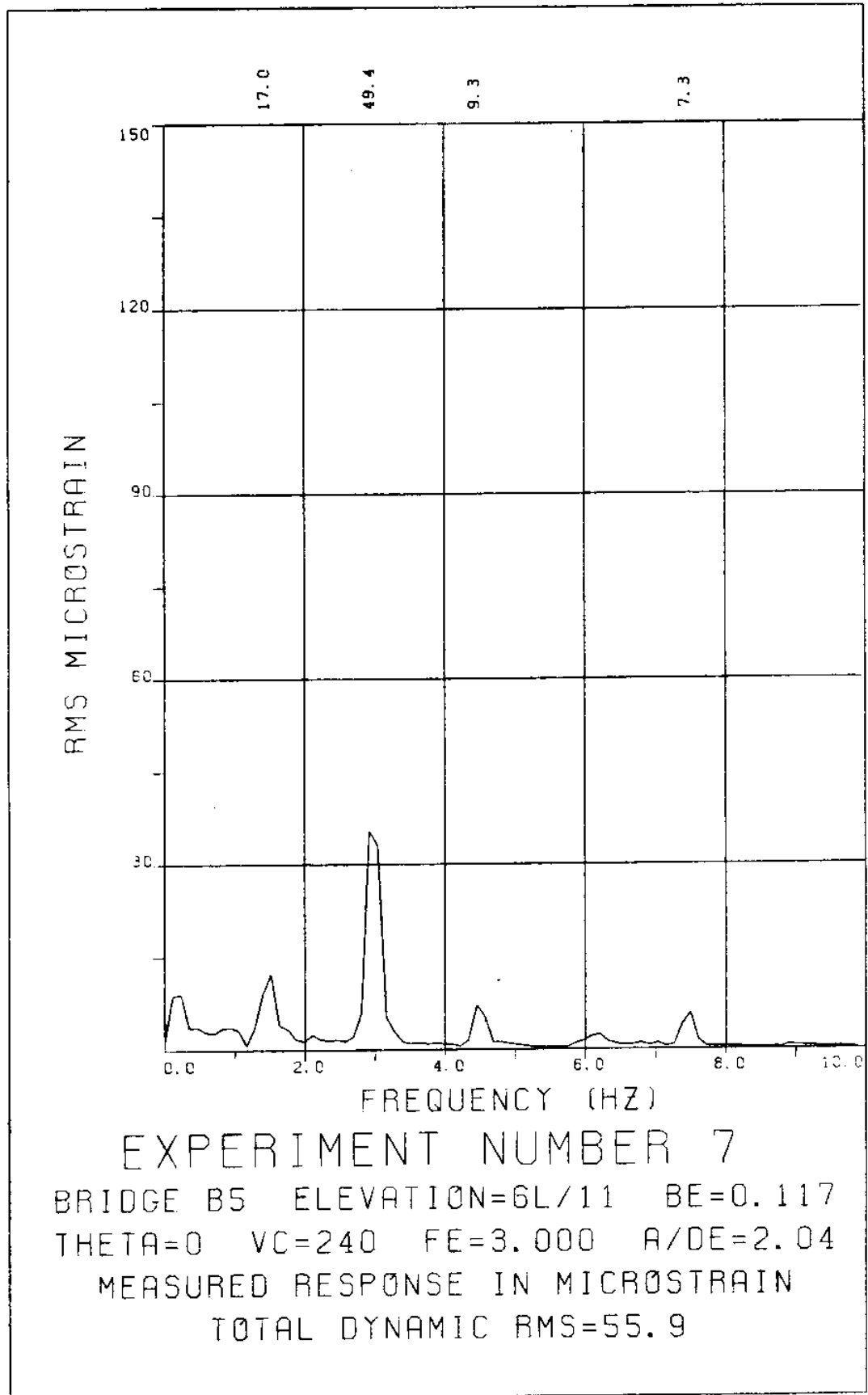
EXPERIMENT NUMBER 7

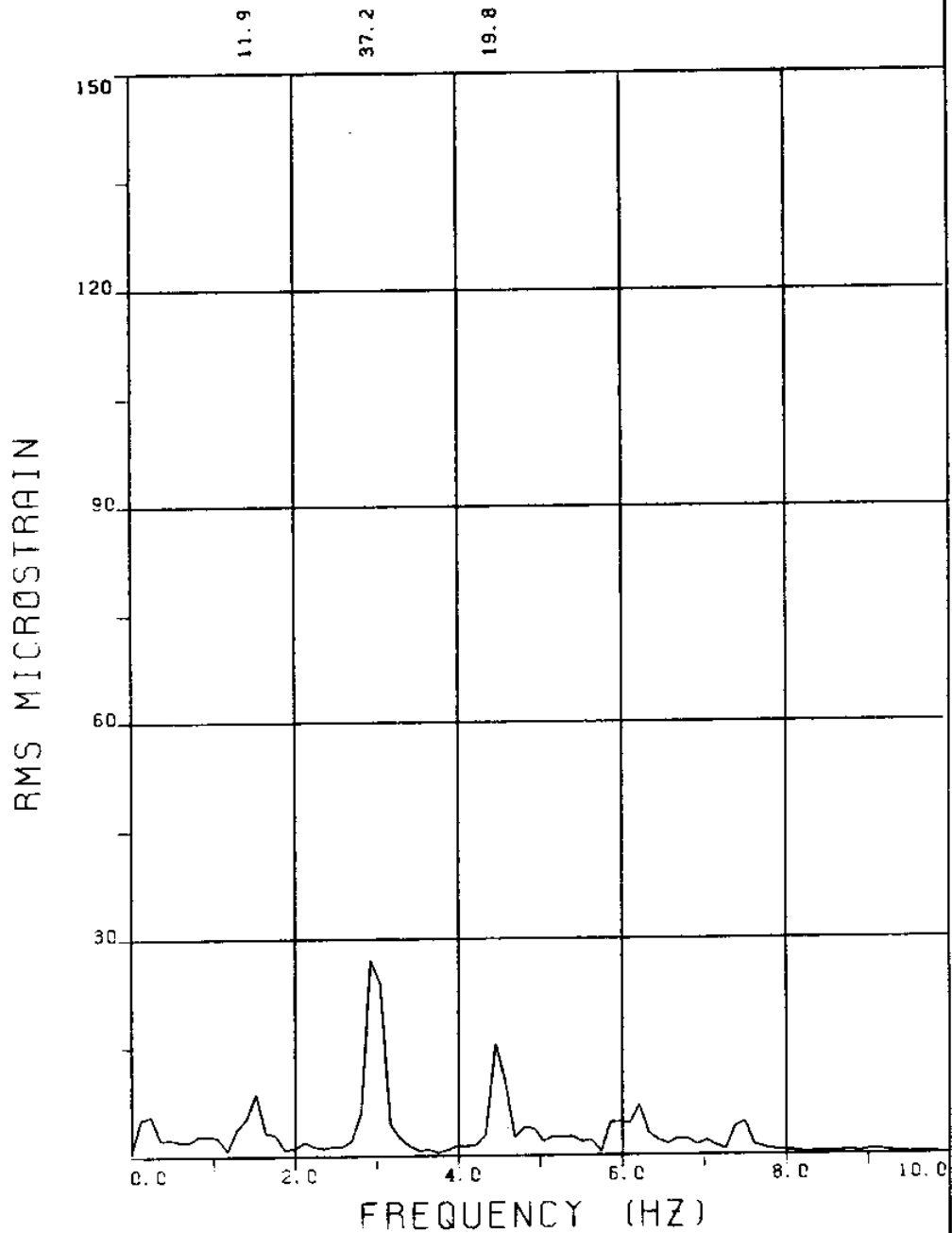
BRIDGE B8 ELEVATION=3L/11 BE=0.117

THETA=0 VC=240 FE=3.000 A/DE=2.04

MEASURED RESPONSE IN MICROSTRAIN

TOTAL DYNAMIC RMS=57.0





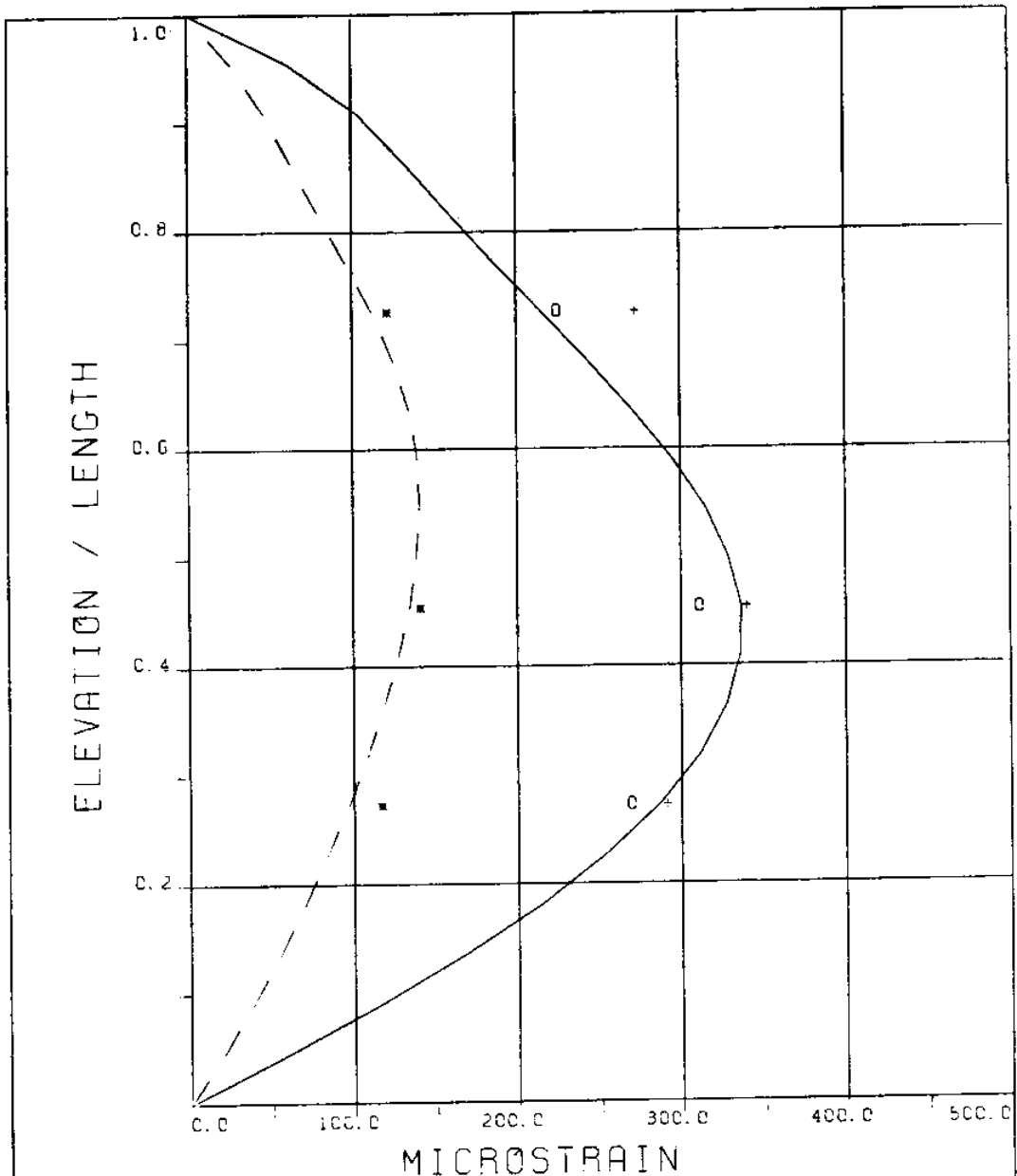
EXPERIMENT NUMBER 7

BRIDGE B3 ELEVATION=8L/11 BE=0.117

THETA=0 VC=240 FE=3.000 A/DE=2.04

MEASURED RESPONSE IN MICROSTRAIN

TOTAL DYNAMIC RMS=47.3



EXPERIMENT NUMBER 7

THETA=0 VC=240 FE=3.000 A/DE=2.04

STATIC RESPONSE IN PLANE A

----- THEORY * * * EXPERIMENT

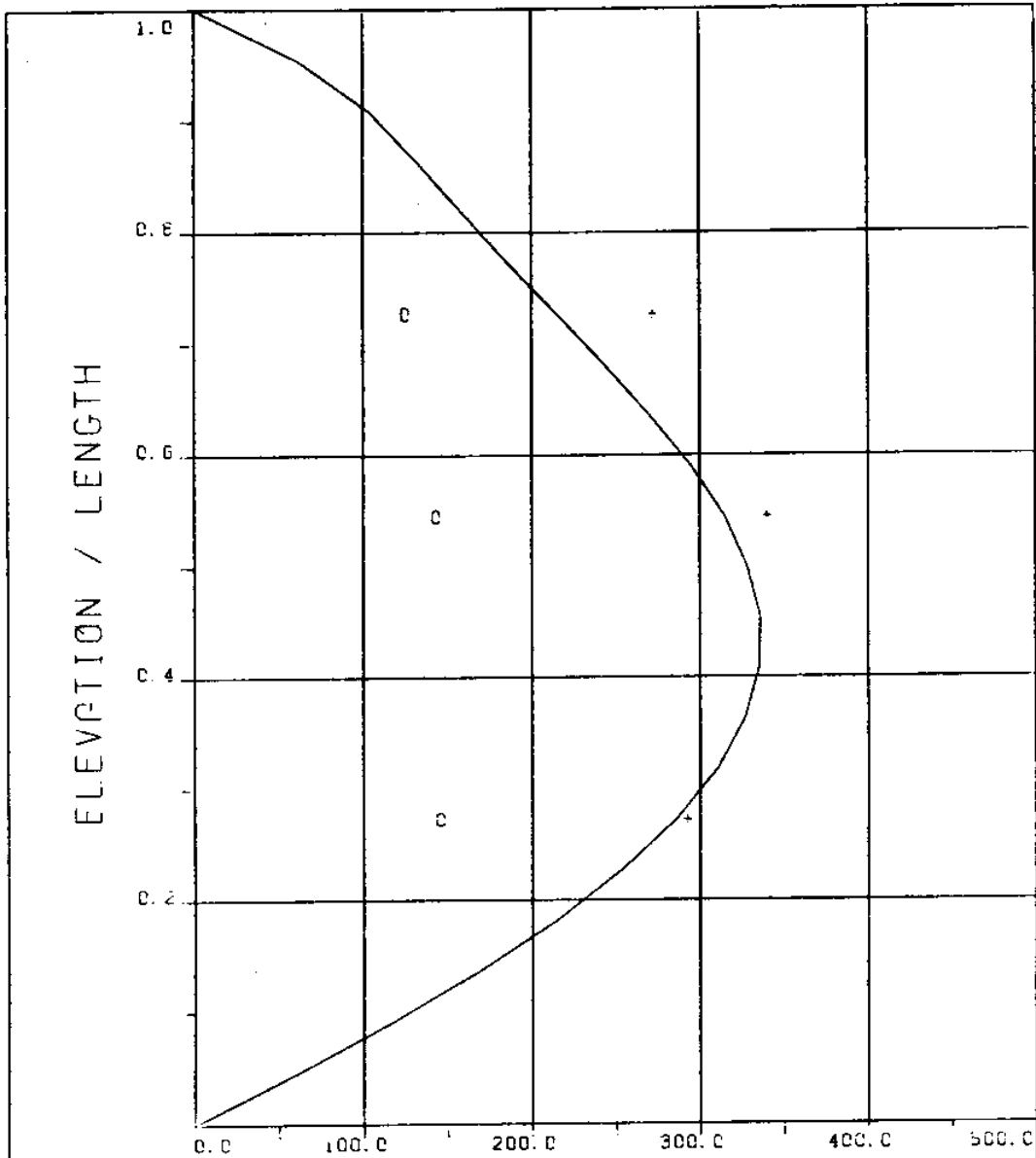
STATIC RESPONSE PLUS DYNAMIC

RESPONSE AT $F = F_E$ IN PLANE A

_____ THEORY o o o EXPERIMENT

MAXIMUM RESPONSE IN PLANE A

_____ THEORY + + + EXPERIMENT



EXPERIMENT NUMBER 7

THETA=0 VC=240 FE=3.000 A/DE=2.04

MAXIMUM DYNAMIC RESPONSE IN PLANE B
 o o o EXPERIMENT

MAXIMUM RESPONSE
 _____ THEORY + + + EXPERIMENT

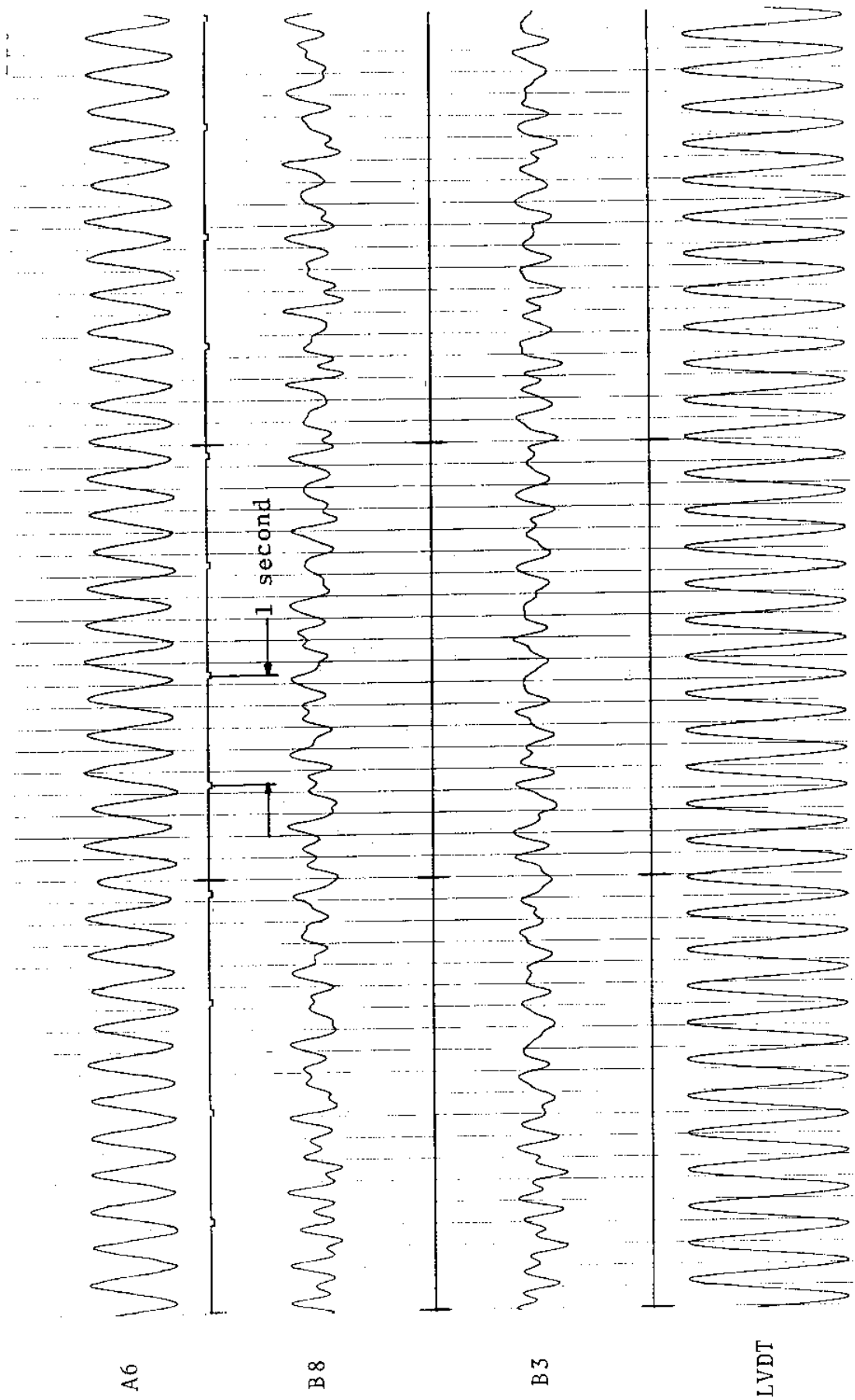


FIGURE 7Ta: LVDT: 0.087 D_e/DIVISION; STRAINS: 15.3 MICROSTRAIN/DIVISION

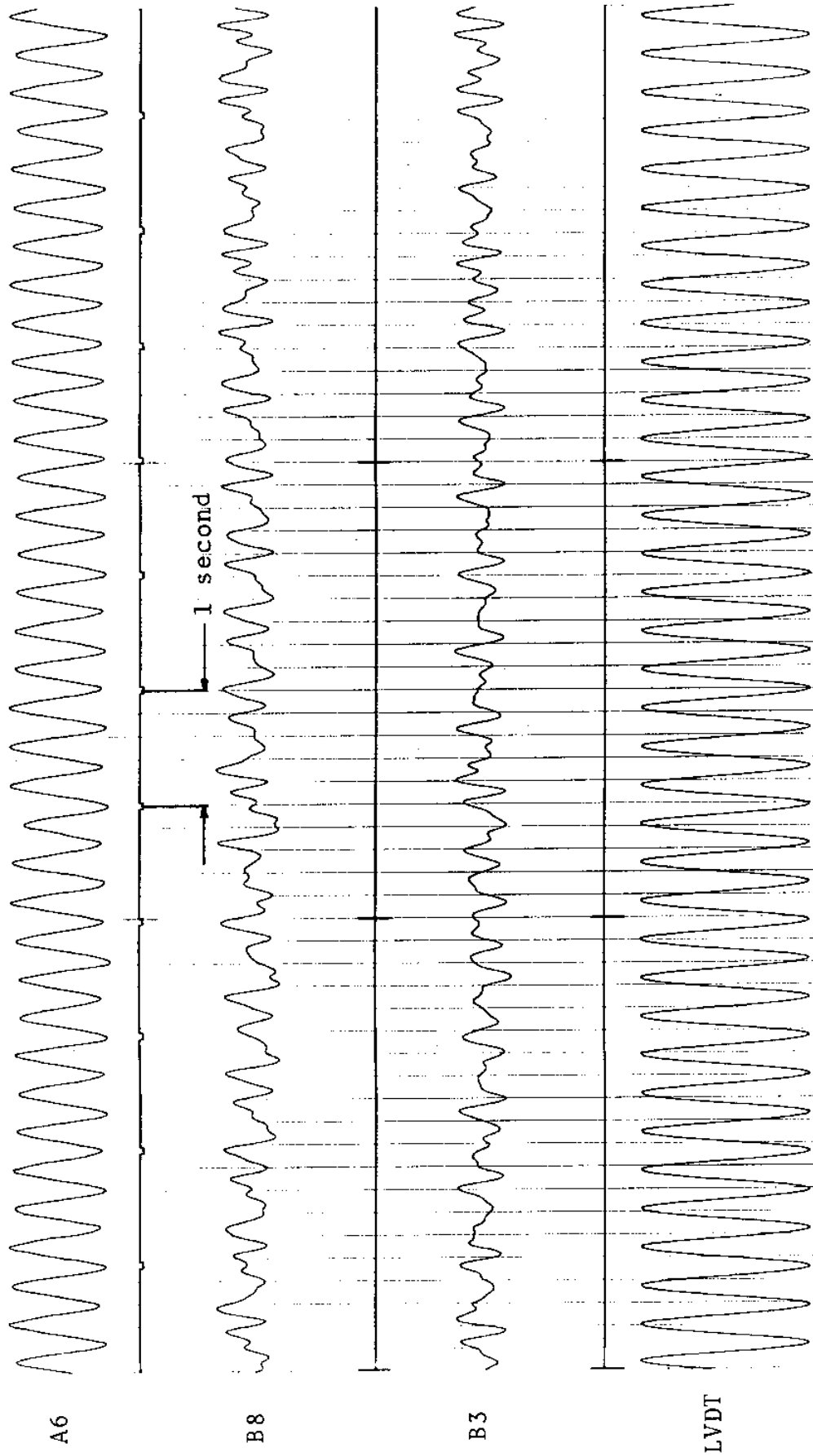


FIGURE 7Tb: LVDT: 0.087 D_e/DIVISION; STRAINS: 15.3 MICROSTRAIN/DIVISION

3. REFERENCES

1. Chrysostomidis, C. and Patrikalakis, N. M., 1982, "An Experimental Procedure for the Prediction of the Dynamic Behavior of Riser Type Systems," Proceedings, 3rd International Conference on the Behaviour of Offshore Structures, August 1982, 565-598, Hemisphere Publishing Co., New York.
2. Chrysostomidis, C. and Patrikalakis, N. M., 1983, Theoretical and Experimental Prediction of the Response of a Marine Riser Model Subjected to Sinusoid Excitation of its Top End With Amplitude of Two Diameters Parallel to a Uniform Stream of Speed Equal to 120 mm/s, MIT Sea Grant Report No. 83-3, Cambridge, MA, 1983.
3. International Mathematical and Statistical Library (IMSL), Reference Manual, 1981, Edition 8, IMSL, Inc.
4. Mercier, J. A., 1973, Large Amplitude Oscillation of a Circular Cylinder in a Low Speed Stream, Ph.D. Thesis, Stevens Institute of Technology, Department of Mechanical Engineering, Ann Arbor, MI: University Microfilms Order No. UM74-884.
5. Patrikalakis, N. M., 1983, Theoretical and Experimental Procedures for the Prediction of the Dynamic Behavior of Marine Risers," Ph.D. Thesis, MIT, Department of Ocean Engineering.
6. Verley, R. L. P. and Moe, G., 1979, The Forces on a Cylinder Oscillating in a Current, Norwegian Institute of Technology, River and Harbour Laboratory, SINTEF Report No. STF60A79061.

I. APPENDIX A

The definitions of c_m and c_d shown in Figures A1 and A2 are given by the following equation:

$$F_x(t) = c_m \rho A_o a + 0.5 c_d \rho D A |A|$$

where

$F_x(t)$ = hydrodynamic force per unit length

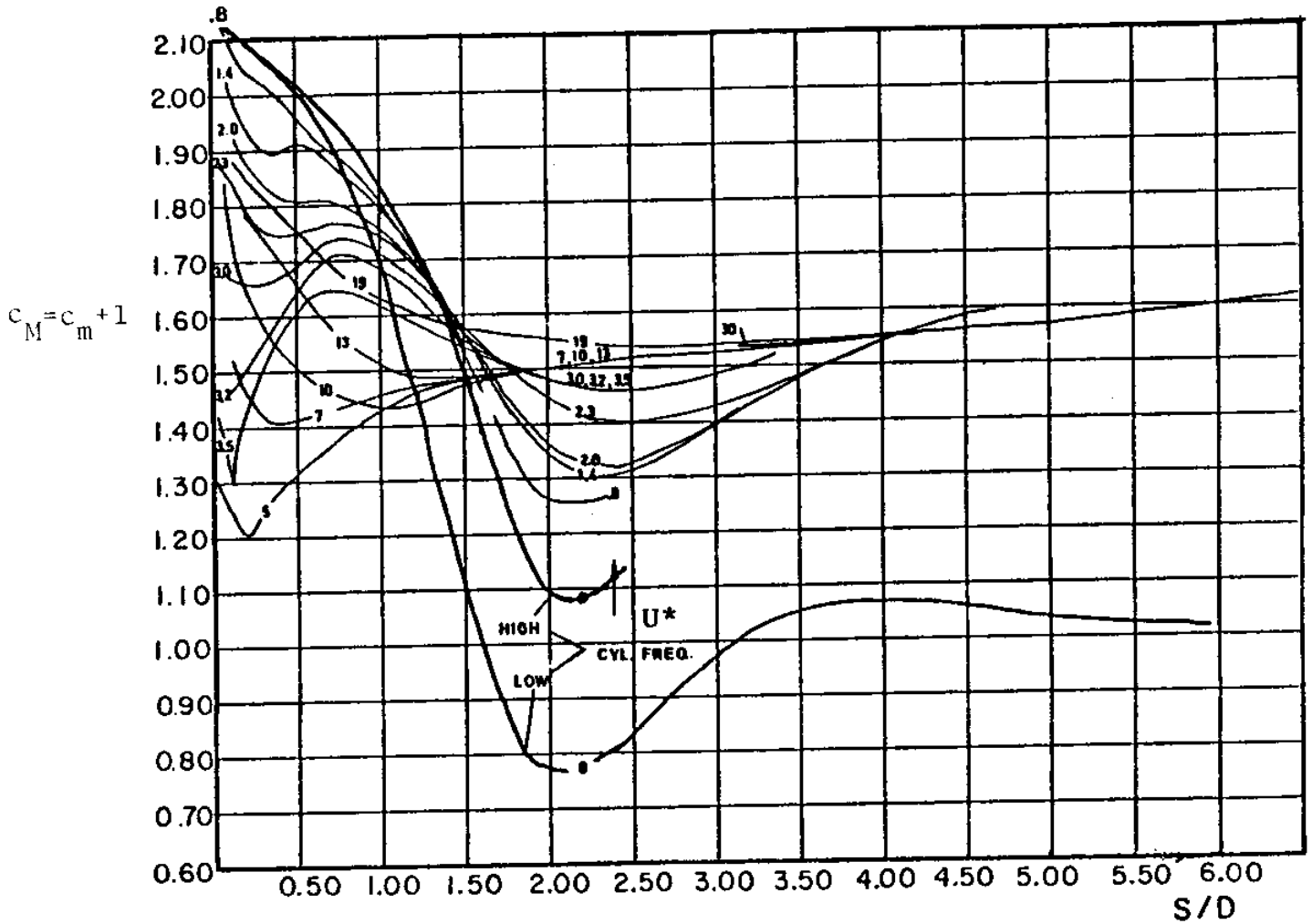
$$A = V_c - r_t$$

$$a = -r_{tt}$$

$$r = \frac{1}{S} \sin \omega t$$

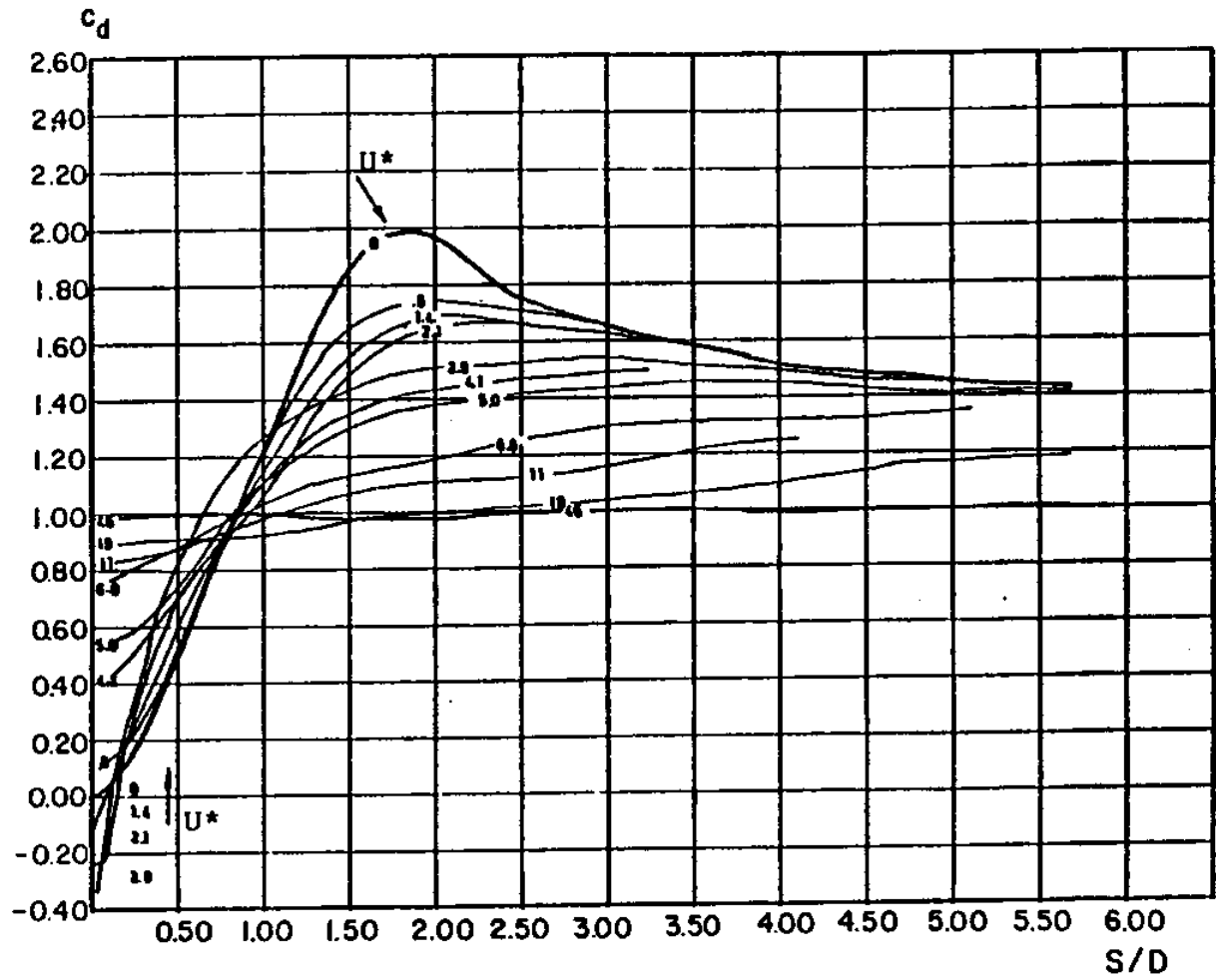
and subscript t denotes differentiation with respect to time.

Figure A-1: Rigid Cylinder Results



Inertia Coefficient $c_M = \text{Amplitude of Inertia Force} / \rho A_0 \omega^2 S + 1$ as a Function of S/D Parametrically with Respect to U^* for Harmonic Oscillations at $\theta=0$ Degrees with Respect to a Current, Verley and Moe (1979).

Figure A-2: Rigid Cylinder Results



Drag Coefficient c_d as a Function of S/D Parametrically with Respect to U^* for Harmonic Oscillations at $\theta=0$ Degrees with Respect to a Current, Verley and Moe (1979).

